Analysis of the effects by signaling inhibitors in the conversion of iPS cells into cancer stem cells

March, 2020

Juan Du

Graduate School of

Natural Science and Technology

(Doctor's Course)

OKAYAMA UNIVERSITY

CONTENTS

CONTENTS

PREFACE

WHO reports, Cancer is a leading cause of death in worldwide, accounting for an estimated 9.6 million deaths in 2018，about 1 in 6 deaths is due to cancer. The most common cancers are: Lung (2.09 million cases), Breast (2.09 million cases), Colorectal (1.80 million cases), Prostate (1.28 million cases), Skin cancer (non-melanoma) (1.04 million cases) and Stomach (1.03 million cases). Meanwhile, the most common causes of cancer death are cancers of: Lung (1.76 million deaths), Colorectal (862, 000 deaths), Stomach (783, 000 deaths), Liver (782, 000 deaths) and Breast (627, 000 deaths). Approximately 70% of deaths from cancer occur in low- and middle-income countries. The economic impact of cancer is significant and is increasing. Therefore, each year billions of funds are allocated towards the research and development of new therapeutic strategies to combat this growing menace. With the advent of new scientific technologies and advancement in molecular cancer research, the future does seem promising. Nevertheless, considerable measures need to be taken in order to solve key issues revolving around this disease such as late presentation of symptoms, development of resistance to available treatments and lack of awareness.

Targeted cancer therapies are drugs or other substances that block the growth and spread of cancer by interfering with specific molecules ("molecular targets") that are involved in the growth, progression, and spread

of cancer. Many different targeted therapies have been approved for use in cancer treatment. These therapies include hormone therapies, signal transduction inhibitors, gene expression modulators, apoptosis inducers, angiogenesis inhibitors, immunotherapies and toxin delivery molecules. They have improved the disease outcomes in many cancer types but still the most serious challenge often encountered in cancer therapy is the development of drug resistance. It is believed that this acquisition of resistance is typically caused by small population of cells in tumor with pre-existing alterations, which can drive the resistance. Since the concept of Cancer stem cells (CSC) has been introduced in late 1990s, its importance in cancer research and development of novel anti-cancer therapies is widely accepted. CSC which are also known as 'tumor initiating cells' represent very small population of tumor sharing common properties with normal stem cells. They are unique cells with self-renewing and tumorigenic potential. Current radio and chemotherapies are able to eliminate the bulk of cancer cells but not cancer stem cells since they are endowed with specific resistance mechanisms. They give rise to new tumors and metastases leading to relapse of the disease. The recurring tumors are more malignant, prone to faster metastasis and exhibits enhanced drug resistance. Overall, this leads to therapy failure reducing the survival rate of cancer patients with specific resistance mechanisms. They give rise to new tumors and metastases leading to relapse of the disease. The recurring tumors are more malignant, prone to faster metastasis and exhibits enhanced drug resistance. Overall, this leads to therapy failure reducing the survival rate of cancer patients.

Previous studies by our group have been investigating the new insight in cancer stem cells (CSCs) by developing a CSC model from mouse and human induced pluripotent stem cells (iPSCs). The novelty of this method was the use of conditioned medium from cancer cell lines to direct the differentiation of iPS towards cancer stem like cells without undertaking any supporting genetic modifications. The evidence of CSCs was widely accepted as small percentage of cell population in tumor that a self-renewal capability and are malignant. Microenvironment is crucial to regulate the proliferation, self-renewal ability and differentiation of normal stem cells.

We established a model of CSCs by culturing mouse induced pluripotent stem cells (miPSCs) in the presence of conditioned medium (CM) of Lewis Lung Carcinoma (LLC) cells. Base on this methodology of developing CSCs from miPSCs, we assessed the risk of carcinogenesis of 110 non-mutagenic chemical compounds, most of which were known as inhibitors of cytoplasmic signaling pathways. We treated miPSCs with each compound for one week in the presence of the CM of LLC cells, while one week was too short for the CM to convert miPSCs into CSCs. As the result, miPSCs treated with PDO325901, CHIR99021 and Dasatinib respectively were found to survive and keep growing while the non-treated miPSCs differentiated and slowed their growth. The survived cells after the treatment exhibited the expression of stemness markers and the spheroid formation in suspension culture indicating that the stemness and the self-renewal capacity were significantly maintained for a week. When the cells were subcutaneously transplanted into

Balb/c nude mice, they formed tumors, which were histopathologically diagnosed malignant. Collectively, we found the three signal inhibitors accelerated the conversion of miPSCs into CSCs. The expression levels of PI3K related genes were assessed and the expression of *pi3kca* was found extensively enhanced 10 to 30 folds of that in miPSCs. Simultaneously, *pik3r5* and *pik3r1* genes were moderately upregulated. These indicated PI3K in either class IA or IB should be enhancing the responsible signaling pathway. Consistently, AKT phosphorylation was found upregulated in the obtained CSCs. Since mTOR expression was recognized in all cells assessed in the experiments, survival of the converted cells might be explained by the sustained pluripotency, which was secured by the expression of stemness markers. Although the mechanism is not clear, inhibition of ErK1/2, tyrosine kinase and/or GSK3-β should closely be involved in the enhancement of PI3K-AKT-mTOR signaling pathway in undifferentiated cells resulting in the sustained stemness, which should lead the conversion into CSCs.

CHAPTER 1

GENERAL INTRODUCTION

1.1 The concept of cancer stem cells

A Russian cell biologist Alexander A. Maximow firstly proposed the concept of stem cell in 1909 (1). In 1961, the two basic features defining stem cells, namely abilities of self-renewal and differentiation into mature cells, were revealed by Till and McCulloch (2). Cancer stem cells (CSCs) were first identified in the granulocytes of acute myeloid leukemia (AML) in 1994 (3). Studies have demonstrated that the CSCs exist in various types of cancers, including breast, brain, lung, gastric, colorectal and so on (4), since 1997 when Bonnet and Dick identified the cancer stem cells by the ability of self-renewal from heterogeneous tumor xenograft (5). CSCs has been indicated a subpopulation of stem-like cells within tumors, which exhibit characteristics of both stem cells and cancer cells. In addition to self-renewal and differentiation capacities, CSCs have the ability to form tumors when transplanted into an animal host.

Currently, with the development of new technologies and advanced technologies, research on cancer has undergone tremendous changes. These have significantly improved our understanding of the molecular and cellular mechanisms of cancer progression, but how tumors evade treatment remains elusive. CSCs are nowadays generally considered to represent a unique population of cancer cells that are tumorigenic and resistant to most chemotherapeutic agents and radiation therapy supporting cancer progression and recurrence.

1.2 The function of Cancer Stem Cells

1.2.1 Key Signaling Pathways Regulation of Cancer Stem Cells

The self-renewal and differentiation of CSC is tightly controlled by multiple regulatory networks, many researchers are focusing on the mechanism of the maintenance of CSC from the cancer cell microenvironment. The function of several signaling pathways control cancer, including the Hedgehog, Notch, and Wnt/β-catenin pathway have been previously reviewed (6,7).

Wnt signaling pathway plays an important role in regulating developmental processes and in regulating function of stem cell (8). In classical Wnt signaling pathway, Wnt binding to frizzled (Fzd) receptor activates disheveled (Dsh), inactivating GSK-3β, stabilizing β-catenin, and thereby inducing target genes, including cyclin D1. A second type of receptor related to the low-density lipoprotein (LDL) receptor, known as LRP 5/6, also binds Wnt, together inducing classical Wnt-β-catenin signaling. Dickkopf binds to and represses LRP. In non-classical, Wnt signaling, Wnt binds Fzd and glypican to activate Dsh and thereby Rho and JNK or Ca^{2+}influx, NFAT, PKA and CamkII. An additional non-canonical pathway relevant to this review is the planar cell polarity pathway (PCP) which drives symmetric cell division by enhancing planar polarization of stem cells (9, 10).

The activation of Notch signaling pathway contributes to expansion of a variety of stem and early progenitor cells (11). Notch receptors are single pass

transmembrane proteins. The receptor is processed and cleavage, producing a glycosylated Ca^{2+}stabilized heterodimer. The processed receptor is translocated to the membrane where it binds ligands, members to the Delta-like and Jagged family, located in the signal-sending cells.

Hedgehog signaling is an evolutionarily-conserved pathway essential for self-renewal and cell fate determination. Hedgehog coordinates organismal development and expansion of tissue progenitor or stem cells (12). The Hedgehog ligand is translated as a precursor, which undergoes autocatalytic processing to form an N-terminal fragment (HWN). Secretion and paracrine signaling requires participation of the Dispatched proteins. HhN (including Indian hedgehog (Ihh), desert hedgehog (Dhh), and Sonic hedgehog (Shh)) bind the patched receptor (PTCH1), depressing its constitutive repression of smoothened (Smo), leading to activation of the Gli transcription factors. Compounds targeting this pathway to regulate stem cell function include cyclopamine, vismodegib, itraconazole, antibodies to PTCN and Gli3 and arsenic trioxide which interferes with Gli function. Gross talk between the Notch and Wnt pathway and with receptor tyrosine kinase (RTK) coordinate interactions between growth factor receptor signaling and stem cell expansion.

1.2.2 miRNA regulations of Cancer Stem Cells

miRNAs regulate CSC self-renewal, differentiation, and tumorigenesis, and play an essential role in establishing ESC identity (13). They also play important functional roles in the establishment and maintenance of a core network of

transcription factors and RNA binding proteins (*OCT4*, *Sox2*, *Nanog*, *Klf4*, *c-Myc*, *Tcf3*, *Lin28*) that ensure ESC identity. Several of these factors occupy the regulatory region of a cluster of miRNA that regulate their abundance in a coordinated manner in ESCs (14). The ESC miRNA maintains the ESC program by inhibiting the epigenetic silencing of pluripotency factors Let-7 miRNA opposes the function of ESC miRNA by repression common target genes activated by ESC miRNA. A CSC-specific miRNA expression profiles have been previously reported.

The miRNA circuitry of ESC includes miRNA promoting pluripotency (miR-290, 302, 371 families), are induced by pluripotency transcription factors (*Oct*, *Sox2*, *Nanog*, *Tcf3*, *Kfl4*), which also induce Lin28 and c-Myc. In contrast, proliferation or anti-stemness miRNAs (miR-134, miR296, miR-200c, miR-203, miR-183 and Let7 miRNAs) oppose the action of the pluripotent ESC miRNA (15). Although sharing many phenotypic similarities, significant differences in miRNA profiling has been found between human iPSCs and human ESCs (16-18). In several circumstances, there is some, often limited, overlap between the pluripotent stem cell miRNA signature and cancer stem cell miRNA profiles.

However, there is an important interplay between miRNA and the regulation of factors that govern stemness through heterotypic signals. The tumor microenvironment (immune cells, cancer associated fibroblasts) signals to cancer stem cells. Secreted cytokines and chemokines that may promote stem cell expansion are also regulated by miRNA. miR-17/20 inhibits IL-8 secretion to block

tumor stem cell migration and metastasis. The role of miRNA in regulating heterotypic signaling remains to be further explored.

1.2.3 CSC and Cancer Therapy Resistance

CSC can generate a tumor when transplanted into an immune-deficient animal. Most CSCs are believed to be resistant to chemo- and/or radiation- therapy, indicating the important roles CSCs play in cancer relapse and metastasis. Some breast cancer clinical studies provide clinical evidence for a subpopulation of chemotherapy-resistant CSCs (19, 20). However, there are some publication reported that only a part of patients displayed resistance to chemotherapy due to individual differences in patients (21). Therefore, the clinical application of CSCs in the future will have to account for the differences between individual patients.

1.3 CSC Niche and Metastasis

Niches are specialized microenvironments located within each tissue. The tumor microenvironment or niche is composed of diverse cells each contributing in the maintenance and homeostasis of the neoplastic cells in tumor. Stem cells reside in the niche. Just as the normal stem cells depend on its microenvironment for survival, self-renewal and differentiation CSCs are not autonomous. They require constant input from its surrounding microenvironment or niche. The local tissue environment contributes to the onset and progression of tumorigenesis. The growth factors, cytokines, and small RNAs in the cellular microenvironment are essential for cell nutrition, intercellular communication, signal transduction, and cell fate (22,

23). The mechanism by which the niche regulates CSC self-renewal, differentiation, tumorigenesis and metastasis is of fundamental importance. Metastasis is a complex process by which primary solid tumor cells invade adjacent and distant tissues and grow into secondary tumors. Pre-metastatic niche formation may be an initial event of metastasis.

1.4 Clinical relevance

In recent years, CSCs are a novel cancer target. The gold standard for CSCs is the regeneration of a tumor that resembles the original tumor from which the CSCs was derived. However, a lack of correlation between the proportion of CSCs and clinical outcome restrains the translational application of targeting CSCs. CSCs may have the ability to resist current cancer therapies, resulting in the recurrence and metastasis of cancer. It has also been hypothesized that the proportion of CSCs within a tumor may correlate with the severity of the cancer (24). However, more clinical evidence and research is needed to demonstrate the correlation between the therapy-resistant CSC proportion in a tumor and tumor aggressiveness. Progress in identifying the CSC-specific surface markers, understanding the regulation of CSC tumorigenic capacity, and linking CSC to clinical outcomes will be helpful to drive the therapeutic application of targeting CSCs into the clinic.

Reference

1. Maximow, Alexander A (1909). Der Lymphozyt als gemeinsame Stammzelle der verschiedenen Blutelemente in der embryonalen Entwicklung und im postfetalen Leben der Säugetiere. Folia Haematologica **8**, 125-134.

2. Till, J. E., McCulloch, E. A (1961). A Direct Measurement of the Radiation Sensitivity of Normal Mouse Bone Marrow Cells. Radiation Research 14, **2**, 213.

3. Lapidot T, Sirard C, Vormoor J, Murdoch B, Hoang T, Caceres-cortes J, Minden M, Paterson B, Caligiuri MA, Dick JE (1994). A cell initiating human acute myeloid-leukemia after transplantation into SCID mice. Nature **367**, 645-648.

4. Lee HE, Kim JH, Kim YJ, et al (2011). An increase in cancer stem cell population after primary systemic therapy is a poor prognostic factor in breast cancer. J Br J Cancer **104**, 1730-1738.

5. Bonnet D, Dick JE (1997). Human acute myeloid leukemia is organized as a hierarchy that originates from a primitive hematopoietic cell. Nature Medicine **3**, 730-737.

6. DeSano JT, Xu L. MicroRNA regulation of cancer stem cells and therapeutic implications. AAPS J. 2009; **11**:682-692.

7. Reya T, Clevers H. Wnt signalling in stem cells and cancer. Nature. 2005; **434**:843-850.

8. Clevers H. Wnt/beta-catenin signaling in development and disease.Cell. 2006; **127**:469-480.

9. Le Grand F, Jones AE, Seale V, Scime A, Rudnicki MA. Wnt7a activates the planar cell polarity pathway to drive the symmetric expansion of satellite stem cells. Cell Stem Cell. 2009; **4**:535-547.

10. Von Maltzahn J, Bentzinger CF, Rudnicki MA. Wnt7a-Fzd7 signalling directly activates the Akt/mTOR anabolic growth pathway in skeletal muscle. Nat Cell Biol. 2012; **14**:186-191.

11. Chiba S. Notch signaling in stem cell systems. Stem Cells. 2006; **24**:2437-2447.

12. Peng Y.-C., Levine C.M., Zahid S., Wilson E.L., Joyner A.L. Sonic hedgehog signals to multiple prostate stromal stem cells that replenish distinct stromal subtypes during regeneration. Proc. Natl. Acad. Sci. USA. 2013; **110**:20611-20616. doi: 10.1073/pnas.1315729110.

13. Martinez NJ, Gregory RI. MicroRNA gene regulatory pathways in the establishment and maintenance of ESC identity. Cell Stem Cell. 2010; **7**:31-35.

14. Marson A, Foreman R, Chevalier B, Bilodeau S, Kahn M, Young RA, Jaenisch R. Wnt signaling promotes reprogramming of somatic cells to pluripotency. Cell Stem Cell. 2008; **3**:132-135.

15. Martinez NJ, Gregory RI. MicroRNA gene regulatory pathways in the establishment and maintenance of ESC identity. Cell Stem Cell. 2010; **7**:31-35.

16. Chin MH, Mason MJ, Xie W, Volinia S, Singer M, Peterson C, Ambartsumyan G, Aimiuwu O, Richter L, Zhang J, Khvorostov I, Ott V, Grunstein M, Lavon N, Benvenisty N, Croce CM, Clark AT, Baxter T, Pyle AD, Teitell MA, Pelegrini M, Plath K, Lowry WE. Induced pluripotent stem cells and embryonic stem cells are distinguished by gene expression signatures. Cell Stem Cell. 2009; **5**:111-123.

17. Wilson KD, Venkatasubrahmanyam S, Jia F, Sun N, Butte AJ, Wu JC. MicroRNA profiling of human-induced pluripotent stem cells. Stem Cells Dev. 2009; **18**:749-758.

18. Neveu P, Kye MJ, Qi S, Buchholz DE, Clegg DO, Sahin M, Park IH, Kim KS, Daley GQ, Kornblum HI, Shraiman BI, Kosik KS. MicroRNA profiling reveals two distinct p53-related human pluripotent stem cell states. Cell Stem Cell. 2010; **7**:671-681.

19. Li X, Lewis MT, Huang J, Gutierrez C, Osborne CK, Wu MF, Hilsenbeck SG, Pavlick A, Zhang X, Chamness GC, Wong H, Rosen J, Chang JC. Intrinsic resistance of tumorigenic breast cancer cells to chemotherapy. J Natl Cancer Inst. 2008; **100**:672-679.

20. Meirelles K, Benedict LA, Dombkowski D, Pepin D, Preffer FI, Teixeira J, Tanwar PS, Young RH, MacLaughlin DT, Donahoe PK, Wei X. Human ovarian cancer stem/progenitor cells are stimulated by doxorubicin but inhibited by Mullerian inhibiting substance. Proc Natl Acad Sci U S A. 2012; **109**:2358-2363.

21. Zielske SP, Spalding AC, Wicha MS, Lawrence TS. Ablation of breast cancer stem cells with radiation. Transl Oncol. 2011; **4**:227-233.

22. Zhang Y, Liu D, Chen X, Li J, Li L, Bian Z, Sun F, Lu J, Yin Y, Cai X, Sun Q, Wang K, Ba Y, Wang Q, Wang D, Yang J, Liu P, Xu T, Yan Q, Zhang J, Zen K, Zhang CY. Secreted monocytic miR-150 enhances targeted endothelial cell migration. Mol Cell. 2010; **39**:133-144.

23. Khaled WT, Read EK, Nicholson SE, Baxter FO, Brennan AJ, Came PJ, Sprigg N, McKenzie AN, Watson CJ. The IL-4/IL-13/Stat6 signalling pathway promotes luminal mammary epithelial cell development. Development. 2007; **134**:2739-2750.

24. Diehn M, Clarke MF. Cancer stem cells and radiotherapy: new insights into tumor radio-resistance. J Natl Cancer Inst. 2006; **98**:1755-1757.

CHAPTER 2

Assessed the risk of carcinogenesis of non-mutagenic chemical compounds during the Conversion of iPSCs into CSCs

Abstract

In the present chapter, a model of CSC was evaluated from iPSCs with the effect of cancer cells derived conditioned medium. Making use of the procedure of developing CSCs, we tried to assess the effect of various non-mutagenic chemical compounds that are inhibiting various signaling pathways on the conversion of iPSCs to CSCs. As the result, we found that some inhibitors such as GSK-3β and MEK were enhancing the development of CSCs. The exposure of these inhibitors in the presence of conditioned medium exhibited some significant changes in phenotypes that are the maintenance of stemness, sphere forming ability and the malignant tumorigenesis in vivo. The gene expression profiling by microarray analysis implied that the inhibitors affected the pathways related with cancer development and poor prognosis. We report in this study that the inhibitors have tuning effect on the development of CSCs under the condition provided by the conditioned medium from cancer derived cells.

2.1 Introduction

Chemical compound has been well known for their carcinogenicity, which are evaluated by various assays such as mutagenicity test, repeated dose toxicity study, employing different statistical analysis. However, in recent cancer research, the tumor and their diseased tissues are not only by the uniform cell aggregation of specific gene mutation, but the heterogeneous cell populations, and cancer stem cells induced by cancer niche (Fig. 2.1). We are proposing here the necessity to assess the inducibility of miPSCs to CSCs with chemical compounds.

CSCs has been indicated a subpopulation of stem cells within tumors, which exhibit characteristics of both stem cells and cancer cells. The CSCs are considered to significantly be responsible for growth, metastasis, invasion and recurrence of all cancer. CSCs are typically characterized by continuous proliferation and self-renewal while stem cells are considered to differentiate into tissue specific phenotype of mature cells under the influence of microenvironment. CSCs which is the main cause of cancer recurrence and malignant transformation. CSCs can be traced back to the stem cell lineage which under the influence of a microenvironment, the 'cancer niche', induces malignant tumor. The underlying mechanisms of such switching in the cells are not clear because of the major challenges in isolating CSCs. Moreover, there is no established method for anti-CSC drug screening. On the other hand, we established CSCs derived from miPSCs using conditioned medium collected from cancer cells. In this study, we aim to develop a novel method to evaluate the inducibility of miPSCs to CSCs with chemical compounds, and anti-CSC properties of drugs in vitro.

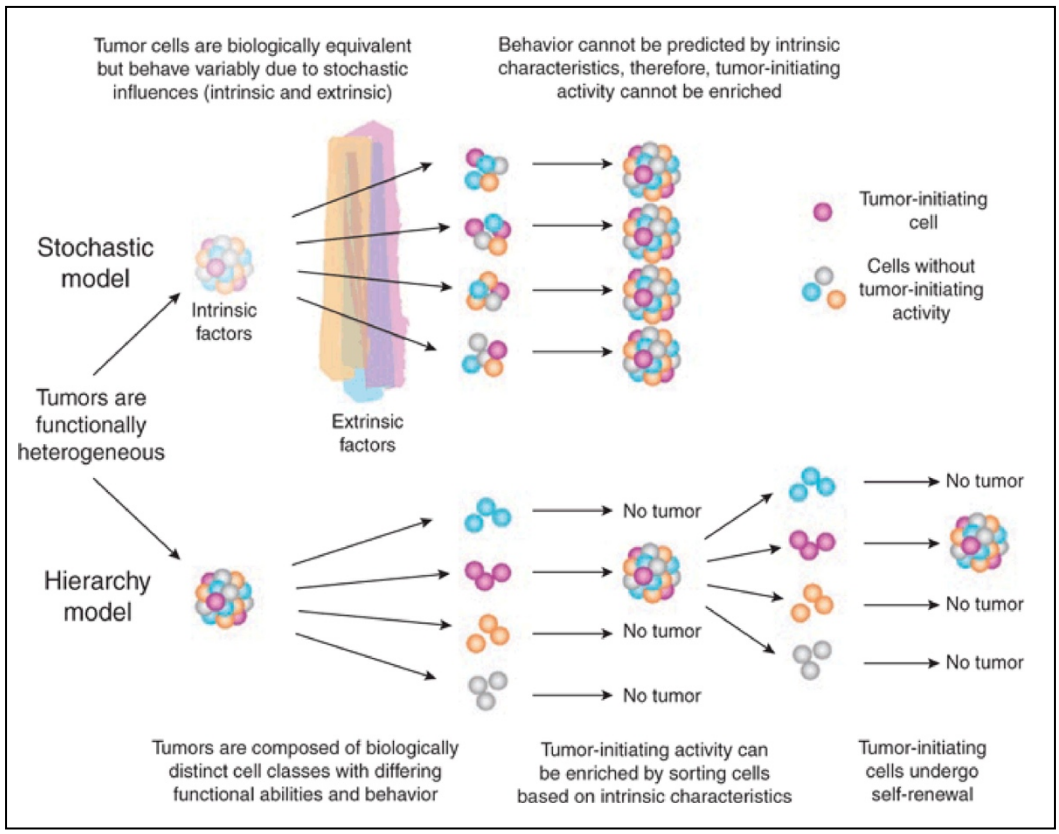

Figure 2.1 Models of tumor heterogeneity.

Courtesy: J.E Dick. Looking ahead in cancer stem cells research. Nature Biotechnology, 27:44-46. 2009

2.2 Results

2.2.1 Risk assessment of carcinogenicity by chemical compounds

Our group previously established a model of CSC cells by culturing mouse iPS cells (miPSCs) in conditioned medium (CM) from mouse cancer cell lines (1-3). On the basis of the previously established protocol, we generated CSC-like cells by culturing miPSCs with conditioned medium for a period of four weeks. Hence, the procedure of developing CSC cells from miPSCs were used to assess the effect of various non-mutagenic 110 chemical compounds in mediating the conversion of miPSCs to CSC cells (Tab. 2.2).

2.2.2 Microscopic evaluation of cell plasticity

Using miPSCs expressing a gene encoding green fluorescent protein (GFP) under the control of *Nanog* promoter (Nanog-GFP miPSCs) (4). Thereby we could distinguish undifferentiated cells from differentiated cells by the presence or absence of GFP expression, respectively. According to this system, conversion into CSC-like cells should keep GFP fluorescence on in the presence of carcinogen. We evaluated the effect of compounds on the conversion of miPSCs cultured with conditioned medium which was collected from Lewis lung carcinoma (LLC) (Fig. 2.2 A). Following a 1-week treatment, the GFP fluorescence of miPSCs persisted during the undifferentiated state, while GFP fluorescence decreased when the miPSCs normally differentiates to die in the absence of Leukemia Inhibitor Factor

(LIF). The miPSCs with conditioned medium without LIF, some of the cells differentiate. Meanwhile, the miPSCs with conditioned medium with compound, we found certain compounds enhanced the expression of GFP in miPSCs while some decreased and others gave no significant effect (Fig. 2.2 B). Subsequently, we evaluated each of the 110 candidate compounds to establish the threshold and concentration by detecting the intensity of GFP fluorescence (Fig. 2.2 C; Tab. 2.1).

A

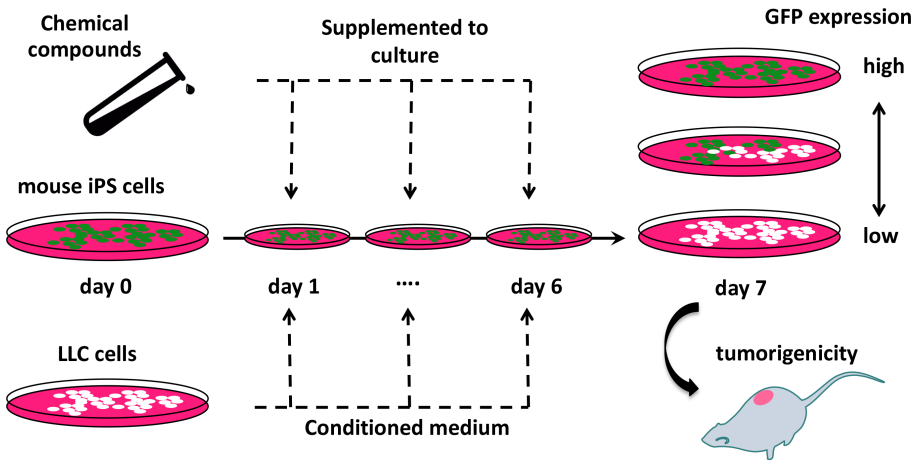
Chemical compounds
Supplemented to culture
GFP expression
high
low
mouse iPS cells
day 0
day 1
....
day 6
day 7
LLC cells
tumorigenicity
Conditioned medium

B

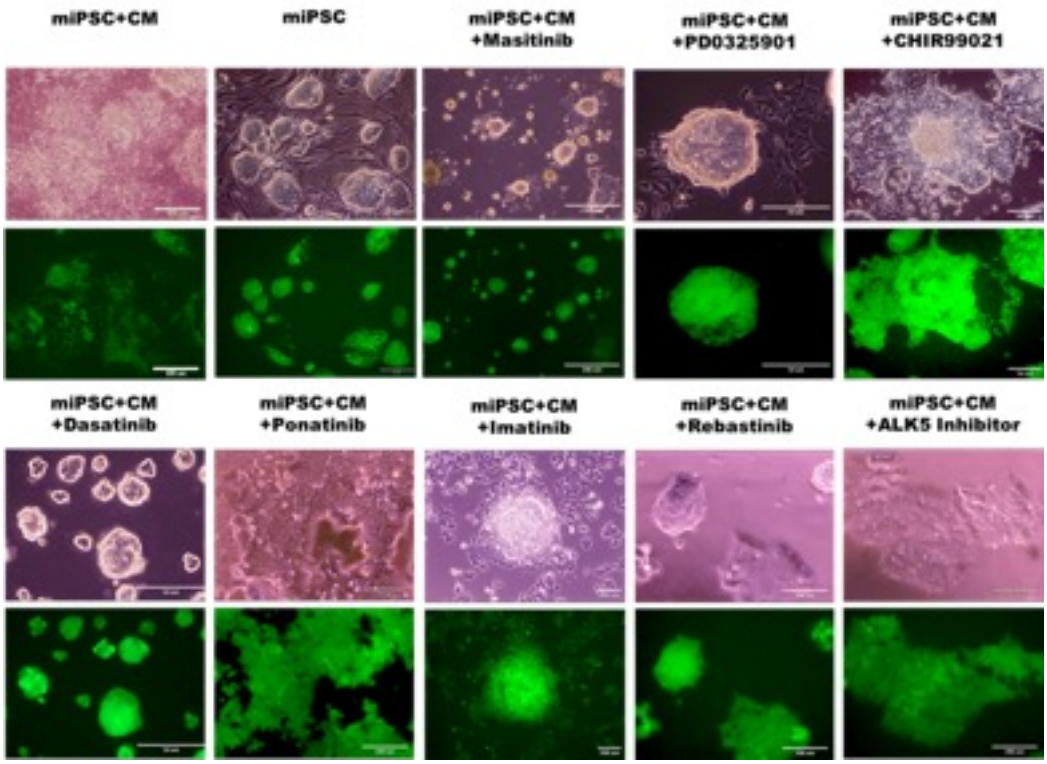
miPSC+CM
miPSC
miPSC+CM +Masitinib
miPSC+CM +PD0325901
miPSC+CM +CHIR99021
miPSC+CM +Dasatinib
miPSC+CM +Ponatinib
miPSC+CM +Imatinib
miPSC+CM +Rebastinib
miPSC+CM +ALK5 Inhibitor

C

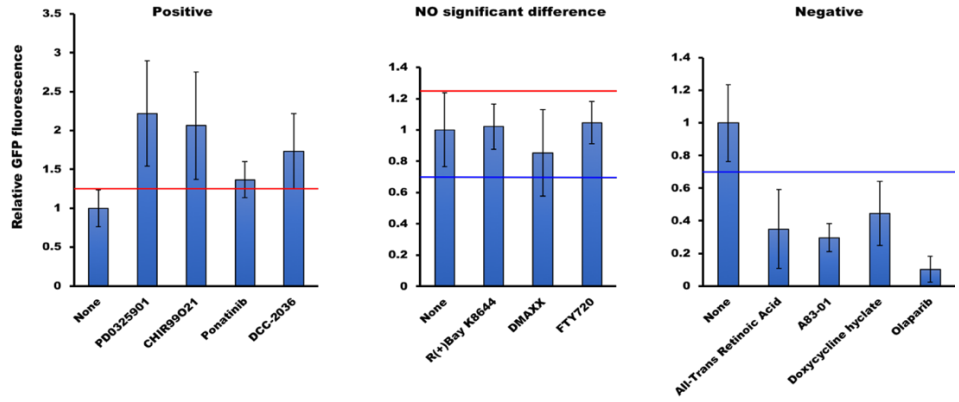

Figure 2.2 The conversion of miPSCs into CSCs accelerlated by the treatments with chemical compounds.

(A) Schematic flow chart of the conversion from miPSCs into CSCs by chemical compounds. (B) Representative images of the conversion from miPS cells into CSCs. Cells were cultured with media containing CM and chemical compound, colonies were observed for the GFP expression after treatment one week. (C) Quantifying the GFP fluorescence to make a threshold to distinguish the compounds.

Table 2.1 Thresholds to distinguish positive and negative results

Results of five standard experiments without inhibitors											
Exp.	**No. 1**		**No. 2**		**No. 3**		**No. 4**		**No. 5**		Overall
	GFPi[*1] *X10*^{3}	RFi[*2]	*GFPi* *X10*^{3}	RFi	*GFPi* *X10*^{3}	RFi	*GFPi* *X10*^{3}	RFi	*GFPi* *X10*^{3}	RFi	
	6.58	0.89	*8.43*	1.01	*6.59*	0.85	*9.03*	1.22	*9.08*	1.24	
	6.97	0.94	*13.88*	1.66	*10.16*	1.31	*7.03*	0.95	*10.3*	1.41	
	8.24	1.12	*6.39*	0.77	*8.05*	1.04	*5.63*	0.76	*6.16*	0.84	
	9.53	1.29	*5.71*	0.68	*5.76*	0.74	*7.08*	0.96	*7.38*	1.01	
	5.7	0.77	*7.41*	0.89	*10.12*	1.3	*8.61*	1.17	*5.79*	0.79	
	7.27	0.98	*8.33*	1	*6*	0.77	*6.92*	0.94	*5.21*	0.71	
average[*3]	*7.38*	1	*8.36*	1	*7.78*	1	*7.38*	1	*7.32*	1	1
error	*1.34*	0.18	*2.91*	0.35	*1.99*	0.26	*1.24*	0.17	*2*	0.27	0.24[*4]

GFP fluorescence intensity (GFPi*1) depicted the read from each well of miPSCs present in CM and the average of the reads were calculated for each experiment. Then the relative fluorescence intensity (RFi*2) was depicted in the table after division by each average value*3. From the table above the thresholds to distinguish the results were determined as 1.00+0.24*4 to show the following: positive > 1.24; 0.76 ≤ no significant difference ≤1.24; negative < 0.76.

Table 2.2 The list of chemical compounds (110)

Name	CAS No.	Company	Target of signaling pathway	GFP fluorescence (P, N, NSD)	optimal concentration (μM)
Masitinib	790299-79-5	AdooQ BioScience	Kit, PDGFα/β	P	6.25
Quizartinib	950769-58-1	AdooQ BioScience	FLT3	P	1.25
Alk5 Inhibitor II	446859-33-2	STEMGENT	TGF-β	P	10
Bafetinib (INNO-406)	859212-16-1	Selleck Chemicals	BCR/ABL	P	1.25
BIRB-796	285983-48-4	AdooQ BioScience	p38-MAPK	P	5
CHIR99021	252917-06-9	Selleck Chemicals	GSK3	P	2.5
Cycbpamine	4449-51-8	STEMGENT	Hedgehog	P	5
Dasatinib	302962-49-8	AdooQ BioScience	BCR/ABL, Src	P	1.25
DCC-2036 (Rebastinib)	1020172-07-9	Selleck Chemicals	Src, ABL1	P	2.5
DMAXX (vadimezan)	117570-53-3	Selleck Chemicals	VDAs	P	0.63

Fingolimod (FTY720)	162359-56-0	Selleck Chemicals	TGF–β	P	1
GZD824	1421783-64-3	Selleck Chemicals	BCR/ABL	P	0.63
imatinb mesylate	220127-57-1	Selleck Chemicals	BCR/ABL	P	25
Imatinib	152459-95-5	AdooQ BioScience	BCR/ABL	P	6.25
KAAD-Cycbpamine	306387-90-6	STEMGENT	GLI1	P	5
PD0325901	391210-10-9	Selleck Chemicals	MEK	P	5
ponatinib	943319-70-8	Selleck Chemicals	ABL, PDGFR, VEGFR, FGFR, Src	P	0.63
R(+)Bay K8644	98791-67-4	Selleck Chemicals	L-type Ca2+ channel activator1,2	P	5
R406	841290-80-0	Cayman Chemical Company	Syk	P	10
Thiazovivin	1226056-71-8	STEMGENT	RHO/ROCK	P	15
2-Methoxyestradiol	362-07-2	Selleck Chemicals	TGF-β	NSD	—
AG-013736	319460-85-0	Selleck Chemicals	VEGFR	NSD	—
AST-487	630124-46-8	Adipogen Life Sciences	FLT3	NSD	—
AT9283	896466-04-9	Selleck Chemicals	Aurora B	NSD	—
AZD-6244/ARRY-886	606143-52-6	Selleck Chemicals	VEGFR	NSD	—

BI-2536	755038-02-9	AdooQ BioScience	Plk1	NSD	—
BIBF-1120 (derivative)	656247-17-5	AdooQ BioScience	VEGFR, PDGF, FGFR	NSD	—
BIBW-2992	850140-72-6	AdooQ BioScience	Her2, EGFR	NSD	—
BIO	667463-62-9	Cayman Chemical Company	GSK3	NSD	—
BIX01294	935693-62-2	STEMGENT	Histone lysine methyltransferase	NSD	—
BMS-345541	547757-23-3	AdooQ BioScience	NF-κB	NSD	—
BMS-387032/SNS-032	345627-80-7	AdooQ BioScience	CDKs	NSD	—
BMS-540215	649735-46-6	AdooQ BioScience	VEGFR	NSD	—
CEP-701	111358-88-4	Focus Biomolecules	FLT3, JAK2, TrkA	NSD	—
CHIR-258/TKI-258	405169-16-6	AdooQ BioScience	FGFR	NSD	—
CHIR-265/RAF-265	927880-90-8	AdooQ BioScience	RAF, VEGFR	NSD	—
CI-1033	289499-45-2	Cayman Chemical Company	ErbBR	NSD	—
Crizotinib	877399-52-5	LC Laboratories, Inc	ALK	NSD	—
Danusertib (PHA-739358)	827318-97-8	Selleck Chemicals	FGFR, ABL	NSD	—

Degrasyn (WP1130)	856243-80-6	Selleck Chemicals	BCR/ABL	NSD	—
DMF	1968/12/2	SIGMA	prepare solution	NSD	—
DMSO	67-68-5	SIGMA	prepare solution	NSD	—
Dorsomorphin	866405-64-3	STEMGENT	AMPK	NSD	—
Doxycycline hyclate	24390-14-5	Selleck Chemicals	Inhibit the inflammatory	NSD	—
Erlotinib	183321-74-6	Cayman Chemical Company	EGFR	NSD	—
FG-4592	808118-40-3	Selleck Chemicals	HIF-PH	NSD	—
Forskolin	66428-89-5	STEMGENT	MAPK	NSD	—
GDC-0879	905281-76-7	AdooQ BioScience	CDK	NSD	—
GDC-0941	957054-30-7	AdooQ BioScience	CLASS I PI3K	NSD	—
Gefitinib	184475-35-2	AdooQ BioScience	EGFR	NSD	—
GSK-690693	937174-76-0	Synkinase Pty Ltd	AK1/2/3	NSD	—
GW-2580	870483-87-7	Cayman Chemical Company	cFMSR	NSD	—
HKI-272	698387-09-6	AdooQ BioScience	EGFR	NSD	—
IDE-1	11160927-48-9	STEMGENT	Inducer ofdefinitive endoderm	NSD	—

IDE-2	N/A	STEMGENT	TGF-β	NSD	—
JNJ-28312141	885692-52-4	AdooQ BioScience	CSF1R	NSD	—
KW-2449	1000669-72-6	AdooQ BioScience	FLT3, STAT5	NSD	—
Lapatinib	231277-92-2	AdooQ BioScience	Her2	NSD	—
LY-317615	170364-57-5	AdooQ BioScience	PKC-β	NSD	—
LY-333531	169939-93-9	Cayman Chemical Company	PKC-β	NSD	—
MLN-120B	783348-36-7	MedChemexpress Co., limited	IKK-β	NSD	—
MLN-518	387867-13-2	AdooQ BioScience	FLT3, cKit, PDGFR	NSD	—
MLN-8054	869363-13-3	AdooQ BioScience	Aurora A	NSD	—
Nilotinib	641571-10-0	AdooQ BioScience	BCR/ABL	NSD	—
PD-173955	260415-63-2	Synkinase Pty Ltd	Src/ Abl	NSD	—
PHA-665752	477575-56-7	AdooQ BioScience	c-Met/HGF/SF	NSD	—
PI-103	371935-79-4	AdooQ BioScience	PI3K	NSD	—
Pifithrin-alpha	63208-82-2	STEMGENT	p53	NSD	—

plinabulin(NPI-2358)	714272-27-2	Selleck Chemicals	Angiogenesis and Tumor vasculature	NSD	—
PLX-4720	918505-84-7	Cayman Chemical Company	B-raf	NSD	—
PP-242	1092351-67-1	AdooQ BioScience	mTOR	NSD	—
PTK-787	212141-51-0	AdooQ BioScience	VEGFR	NSD	—
pumorphamine	483367-10-8	STEMGENT	Hedgehog	NSD	—
R547	741713-40-6	AdooQ BioScience	CDKs	NSD	—
RG108	48208-26-0	STEMGENT	DNA methyltransferase	NSD	—
ROCK II Inhibitor	N/A	STEMGENT	ROCK	NSD	—
Saracatinib (AZD0530)	379231-04-6	Selleck Chemicals	Src	NSD	—
SB431542	301836-41-9	STEMGENT	TGF-β	NSD	—
SC1(Pluripotin)	839707-37-8	STEMGENT	ERK1	NSD	—
SGX-523	1022150-57-7	AdooQ BioScience	MET	NSD	—
Sorafenib	475207-59-1	AdooQ BioScience	VEGFR	NSD	—
Staurosporine	62996-74-1	Cayman Chemical Company	Prevent ATP binding to the kinase	NSD	—
SU-14813	627908-92-3	AdooQ BioScience	VEGFR, PDGF, FGFR	NSD	—

Sunitinib	341031-54-7	Cayman Chemical Company	VEGFR	NSD	—
TAE-684	761439-42-3	Synkinase Pty Ltd	ALK	NSD	—
TG-100-115	677297-51-7	AdooQ BioScience	PI3K	NSD	—
TG-101348	936091-26-8	AdooQ BioScience	JAK	NSD	—
Tranylcypromine	1986-47-6	STEMGENT	MAO	NSD	—
Vandetanib	443913-73-3	Cayman Chemical Company	VEGFR, EGFR	NSD	—
Veliparib (ABT-888)	912444-00-9	Selleck Chemicals	PARP	NSD	—
Wnt inhiitor iwp-2	686770-61-6	STEMGENT	Wnt	NSD	—
Wnt inhiitor iwp-3	N/A	STEMGENT	Wnt	NSD	—
Wnt inhiitor iwp-4	N/A	STEMGENT	Wnt	NSD	—
Y27632	146986-50-7	STEMGENT	ROCK	NSD	—
A-674563	552325-73-2	AdooQ BioScience	PKA, CDK2, AKT	N	12.5
A83-01	909910-43-6	Selleck Chemicals	TGF-**β**, ALK5	N	10
ABT-869	796967-16-3(4)	AdooQ BioScience	RTK, VEGF, PDGF	N	6.25

All-Trans Retinoic Acid	302-79-4	Selleck Chemicals	Ligand for the retinoic acid receptor	N	1
AMG-706	857876-30-3	AdooQ BioScience	VEGFR	N	10
DAPT	208255-80-5	STEMGENT	Notch	N	10
IOX2	931398-72-0	Selleck Chemicals	PHD	N	0.63
IPA3	42521-82-4	STEMGENT	Pak1	N	2.5
LDN-193189	1062368-24-4	STEMGENT	BMP	N	5
Nibtinib (AMN-107)	641571-10-0	Selleck Chemicals	ERK1/2, PDGF	N	0.31
NVP-BHG712	940310-85-0	Selleck Chemicals	RTK	N	15
Olaparib (AZD2281)	763113-22-0	Selleck Chemicals	BRCA1, BRCA2	N	1
PD173034	219580-11-7	STEMGENT	FGFR	N	5
Pifithrin-mu(u)	64984-31-2	STEMGENT	p53	N	10
SMO antagonist	N/A	STEMGENT	Hedgehog	N	5
Tanespimycin (17-AAG)	75747-14-7	Selleck Chemicals	Her2, AKT	N	0.5

P: Positive compound, N: Negative compound, NSD: No Significant Difference compound

2.3 Discussion

The risk assessment of carcinogen for the chemical compound has always been performed by different procedures such as mutagen tests, repeated dose toxicity studies, and statistical analyses. Our group developed a simple and feasible method for the preliminary screening in this study. According to the reports of producing CSCs (1-3), we exploited miPSCs expressing GFP under the control of *Nanog* promoter to assess the risk of generating CSCs for 110 non-mutagenic chemical compounds, most of which were known as inhibitors of cytoplasmic signaling pathways. Since *Nanog* was considered as a marker widely associated with stemness (5, 6), the assessment procedure was designed to observe miPSCs with GFP for 1-week in the presence of each chemical compound. Compared with the control group, the intensity of GFP fluorescence from the miPSCs was monitored to judge the effects of the chemical compounds. Twenty chemical compounds in 110 exhibited significantly enhanced GFP fluorescence. After evaluating the colony forming efficiency, we selected 8 chemical compounds. Then the sphere formation potential, which contributes to the cell stemness maintenance and self-renewal, was successful to select 6. Finally, evaluating the tumorigenic potential, three compounds, PD0325901, CHIR99021 and Dasatinib, were found to facilitate the tumor formation. Taking spheroid formation in the suspension culture and high tumorigenic potential of the resultant cells into consideration as the basic characteristics of CSCs (7-9), we concluded the cells were CSCs converted from miPSCs.

Reference

1. Chen L, Kasai T, Li Y, Sugii Y, Jin G, Okada M, Vaidyanath A, Mizutani A, Satoh A, and Kudoh T, et al (2012). A model of cancer stem cells derived from mouse induced pluripotent stem cells. PLoS One. **7**, e33544.

2. Calle AS, Nair N, Oo AKK, Prieto-Vila M, Koga M, Khayrani AC, Zahra MH, Hurley L, Vaidyanath A, and Seno A, et al (2016). A new PDAC mouse model originated from iPSCs-converted pancreatic cancer stem cells (CSCcm). Am J Cancer Res. **6**, 2799-2815.

3. Nair N, Calle AS, Zahra MH, Prieto-Vila M, Oo AKK, Hurley L, Vaidyanath A, Seno A, Masuda J, and Iwasaki Y, et al (2017). A cancer stem cell model as the point of origin of cancer-associated fibroblasts in tumor microenvironment. Sci Rep. **7**(1),6838.

4. Okita K, Ichisaka T and Yamanaka S. Generation of germline-competent induced pluripotent stem cells. Nature. 2007, **448**:313-7.

5. Mitsui K, Tokuzawa Y, Itoh H. et al (2003). The homeoprotein Nanog is required for maintenance of pluripotency in mouse epiblast and ES cells. Cell **113**, 631-642.

6. Chambers I, Colby D, Robertson M. et al (2003). Functional expression cloning of Nanog, a pluripotency sustaining factor in embryonic stem cells. Cell **113**, 643-655.

7. Ruiz-Vela A, Aguilar-Gallardo C, Simo´n C (2009). Building a framework for embryonic microenvironments and cancer stem cells. Stem Cell Rev **5**, 319-327.

8. Baiocchi M, Biffoni M, Ricci-Vitiani L, Pilozzi E, De Maria R (2010). New models for cancer research: human cancer stem cell xenografts. Curr Opin Pharmacol **10**, 380-384.

9. Miyoshi N, Ishii H, Sekimoto M, Haraguchi N, Doki Y, et al (2010). Properties and identification of cancer stem cells: a changing insight into intractable cancer. Surg Today **40**, 608-613.

CHAPTER 3

Signaling Inhibitors Accelerate the Conversion of miPS Cells into Cancer Stem Cells in Tumor Microenvironment

Abstract

In the present chapter, we treated miPSCs with each compound for 1 week in the presence of a CM of Lewis lung carcinoma (LLC) cells however the 1-week period was too short for the CM to convert miPSCs into CSCs. Consequently, PDO325901 (MEK inhibitor), CHIR99021 (GSK-3β inhibitor) and Dasatinib (Abl, Src and c-Kit inhibitor) were found to confer miPSCs with the CSC phenotype in 1 week. The tumor cells that survived exhibited stemness markers, spheroid formation and tumorigenesis in Balb/c nude mice. Hence, we concluded that the three signal inhibitors accelerated the conversion of miPSCs into CSCs. In the accordance with our previous study, we found that the PI3K-Akt signaling pathway was upregulated in the CSCs. Herein, we focused on the expression of relative genes after the treatment with these three inhibitors. Our results demonstrated an increased expression of *pik3ca, pik3cb*, *pik3r5* and *pik3r1* genes indicating class IA PI3K as the responsible signaling pathway. Hence, AKT phosphorylation was found to be up-regulated in the obtained CSCs. Inhibition of Erk1/2, tyrosine kinase, and/or GSK-3β were implied to be involved in the enhancement of the PI3K-AKT signaling pathway in the undifferentiated cells, resulting in the sustained stemness, and subsequent conversion of miPSCs into CSCs in the tumor microenvironment.

3.1 Introduction

Recent reports have shown that the interaction between non-CSCs and the microenvironment plays a crucial role in promoting the dynamic conversion of non-CSCs into CSCs, which possess hierarchical heterogeneity and plasticity (1-3). Although the factors involved in regulating the conversion have not been identified, epithelial mesenchymal transition (EMT) is considered to be closely related to the presence of CSCs. The phosphoinositide 3-kinase (PI3K), AKT (protein kinase B, PKB) and mammalian target of rapamycin (mTOR), which constitutes the core cascade called the PI3K/AKT/mTOR signaling cascade, are considered to have regulatory roles in cell survival, proliferation, and differentiation, and a critical role in tumorigenesis (4). PI3K is reported to be associated with the development of various human tumors, including breast cancer, lung cancer, melanoma and lymphomas (5-9). Furthermore, the PI3K downstream kinase, AKT, is reported to be involved in malignant transformation (10). In this context, some environmental factors could be important stimulants to understand the mechanism of conversion of non-CSCs to CSCs.

Some chemical compounds are well known as mutagens and/or carcinogens. Some as inhibitors of cytoplasmic signaling pathways. And others as both mutagens and/or carcinogens and inhibitors. Chemical compounds are usually evaluated for their risk to induce cancer by various assays such as mutagenicity assays, repeated dose toxicity studies, and statistical analyses. In our previous study, the conversion of miPSCs into CSCs was demonstrated by the treatment with a conditioned

medium (CM) prepared from different cancer cell lines, for a period of 4 weeks (11-13). This implies that the essential factors should be contained in the CM derived from cancer cells mimicking the tumor microenvironment. In the current study, we proposed a simple method to assess the risks of tumor-inducing factors in the presence of chemical compounds that accelerated the conversion of miPSCs into CSCs. Furthermore, we used the signaling inhibitors to elucidate the signaling pathways responsible for the appearance of CSCs.

3.2 Results

3.2.1 Stemness of GFP positive miPSCs after 1-week treatment

Previous evidence suggests that the ability to form spheroids is associated with CSC properties (14,15). Therefore, GFP-positive cells that survived following a 1-week treatment were further assessed for the sphere-forming potential. We assessed the chemical compounds, which exhibited positive capability to the cell survival following1-week treatment (Tab. 2.1, 2.2), for sphere formation potential in a suspension culture. Our results indicated that six compounds promoted the sphere formation (Fig. 3.1 A-B), while the remaining candidate compounds failed to demonstrate this property. The surviving cells were then cultured in adhesive condition analyzed by Fluorescence Activated Cell Sorter (FACS) and found approximately 60-80% of the cells expressing GFP (Fig. 3.1 C).

We assessed the expression of endogenous stemness markers, *Oct3/4, Sox2, Nanog*, *Klf4* and *c-Myc*, which have a dominant role in the maintenance of ESCs and iPSCs, self-renewal in the surviving cells, using rt-qPCR. The expression level of each endogenous gene and transgene was confirmed by using specific primers (16). The expression of endogenous *Oct3/4, Sox2* and *Nanog* genes was significantly increased in miPSCs treated with Masitinib, PD0325901, CHIR99021 and Dasatinib when compared to miPSCs without treatment (Fig. 3.1 D). As for the *Klf4* gene, only PD0325901, CHIR99021 and Dasatinib increased the expression while Masitinib failed to do so. We did not detect any aberrant activation of the

transgene, pertinent to viral-transduction for establishment of miPSCs (Fig. 3.1 E). Since PD0325901, CHIR99021 and Dasatinib were feasibly enhanced the sphere formation and the expression of stemness marker, we also confirmed the increased expression of *Nanog* and *Oct3/4* by immunoblotting analysis in the presence of PD0325901, CHIR99021 and Dasatinib (Fig. 3.1 F). The amounts of *Nanog* and *Oct3/4* increased in miPSCs when treated with these three compounds. Collectively, PD0325901, CHIR99021 and Dasatinib were confirmed to maintain the stemness of miPSCs.

A

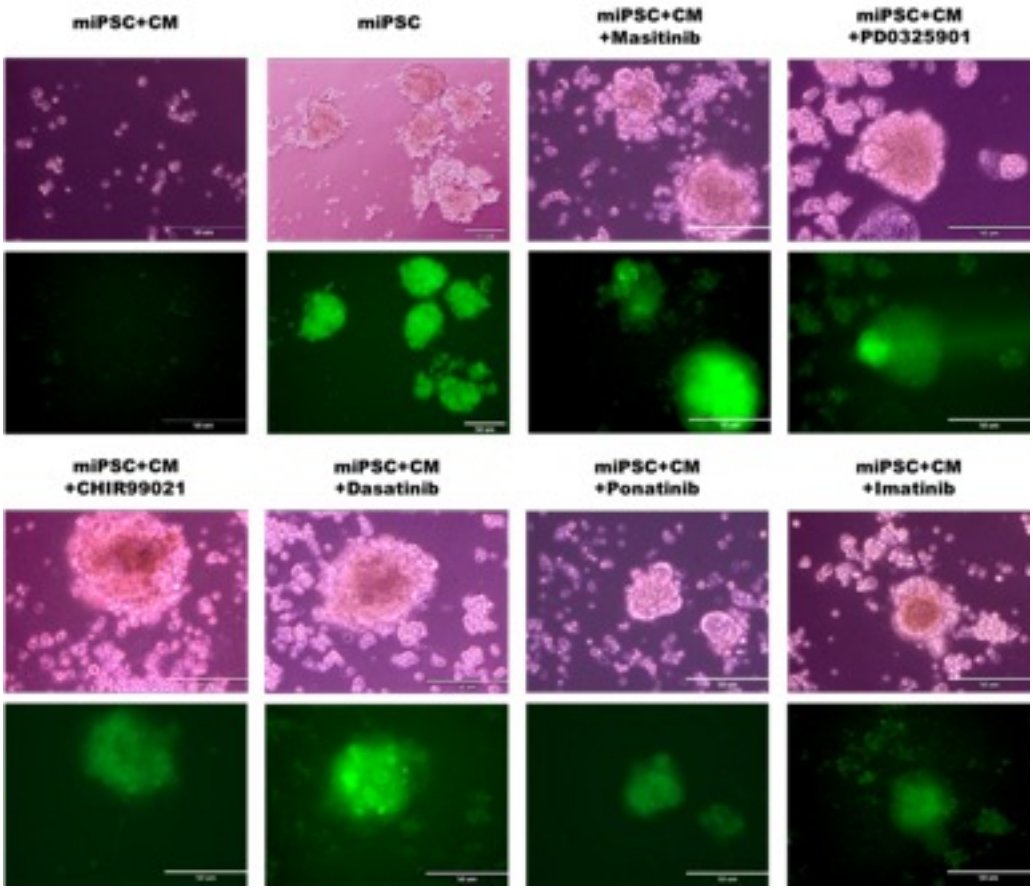
miPSC+CM
miPSC
miPSC+CM
+Masitinib
miPSC+CM
+PD0325901
miPSC+CM
+CHIR99021
miPSC+CM
+Dasatinib
miPSC+CM
+Ponatinib
miPSC+CM
+Imatinib

B

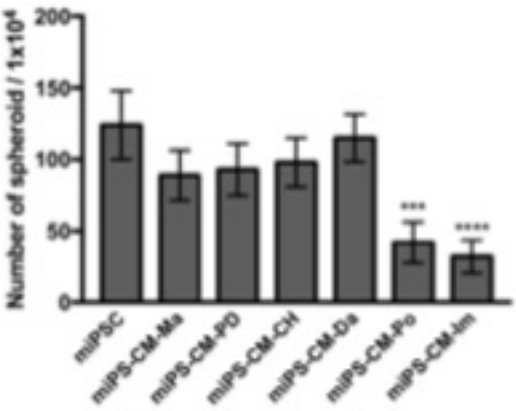
Number of spheroid / 1x10⁴
200
150
100
50
0
***
****
miPSC
miPS-CM-Ma
miPS-CM-PD
miPS-CM-CH
miPS-CM-Da
miPS-CM-Po
miPS-CM-Im

C

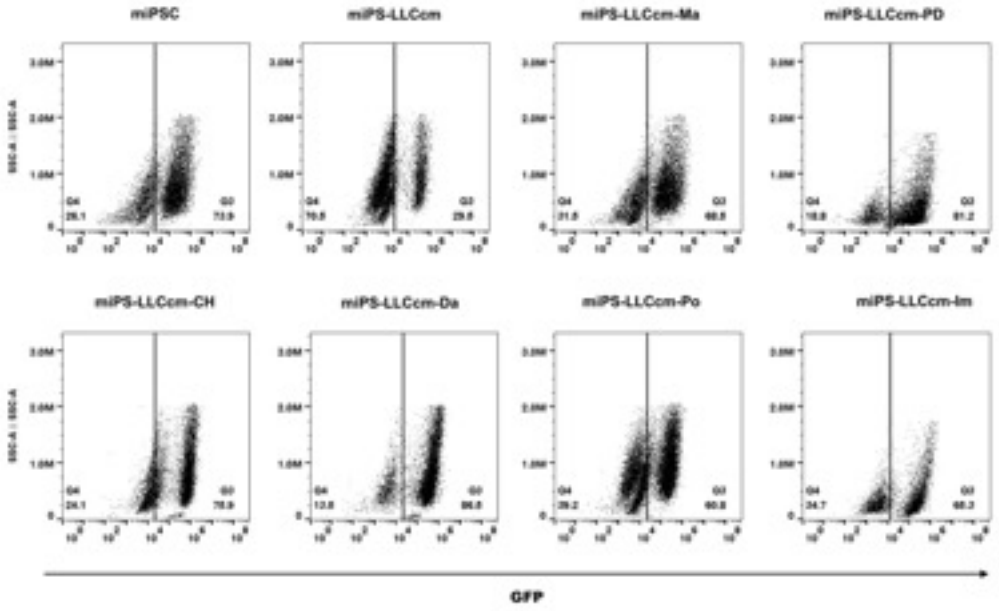
miPSC
miPS-LLCcm
miPS-LLCcm-Ma
miPS-LLCcm-PD
miPS-LLCcm-CH
miPS-LLCcm-Da
miPS-LLCcm-Po
miPS-LLCcm-Im
GFP

D

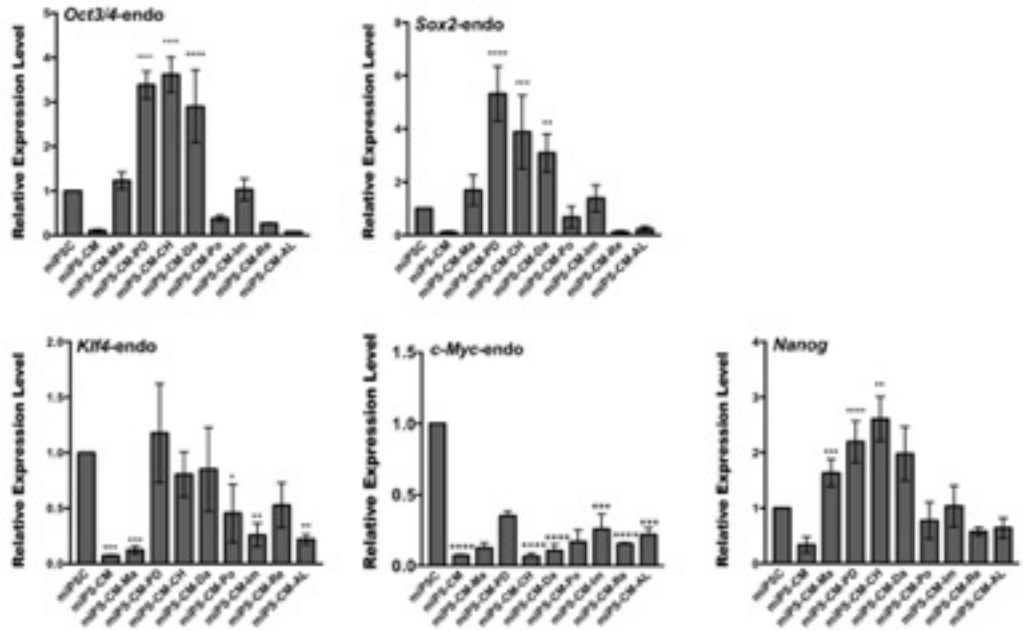
Oct3/4-endo
Sox2-endo
Klf4-endo
c-Myc-endo
Nanog
Relative Expression Level

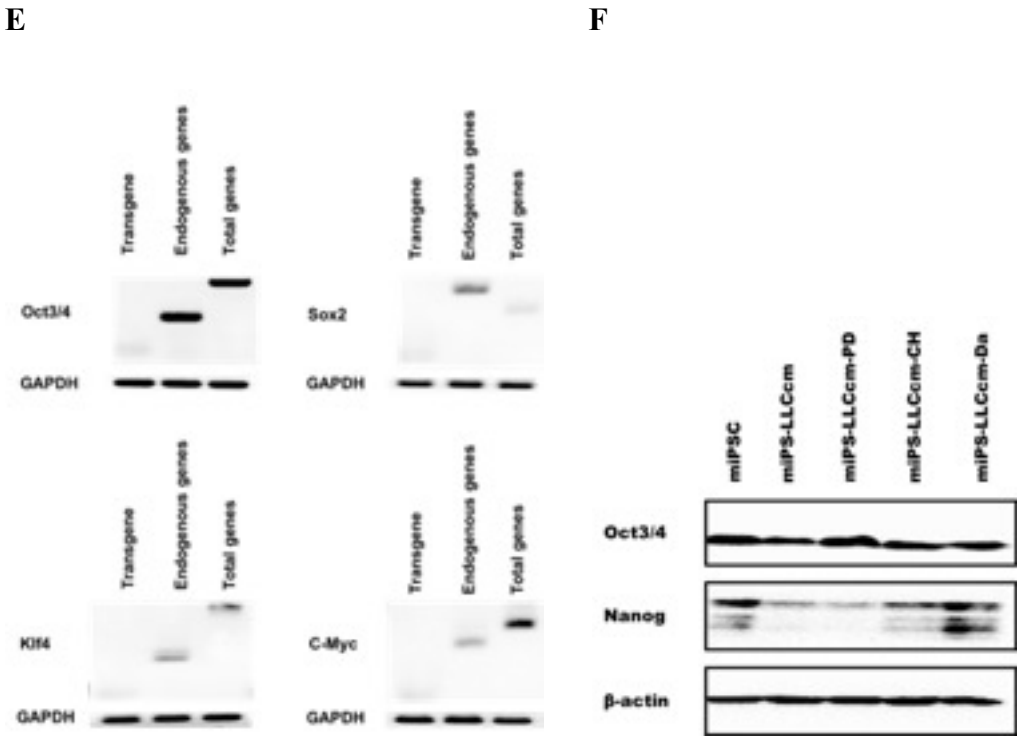

Figure 3.1 Positive chemical compounds promote self-renewal capacity in the conversion of miPSCs into CSCs. (A) Sphere formation assay shows spherogenic potential and the expression of GFP. (B) Graphical representation of the number of spheroids after the conversion of 1-week. (C) FACS analysis shows GFP population in the conversion cells after treated with chemical compounds. (D) The expression levels of stemness markers (endogenous genes) were analyzed by rt-qPCR. The data were analyzed using ordinary one-way ANOVA multiple comparisons and presented as the mean ± standard deviation ****P<0.0001, ***P<0.001, **P<0.01, *P<0.05. (E) Representative agarose gel electrophoresis of PCR products for the detection of stemness markers (endogenous, transgenes and total genes) in miPSCs. (F) Immunoblotting analysis the expression of *Oct3/4* and *Nanog*.

3.2.2 Differentiation potential in converted cells

Differentiation potential is another property of CSCs as well as self-renewal. miPSCs and other three converted cells were assessed for the potential to differentiate into endothelial-like cells forming capillary-like tubes on Matrigel (Fig. 3.2). Capillary-like tubes were confirmed to form by these cells indicating pro-angiogenic properties in tumorigenesis. These cells showed high potential of tube formation.

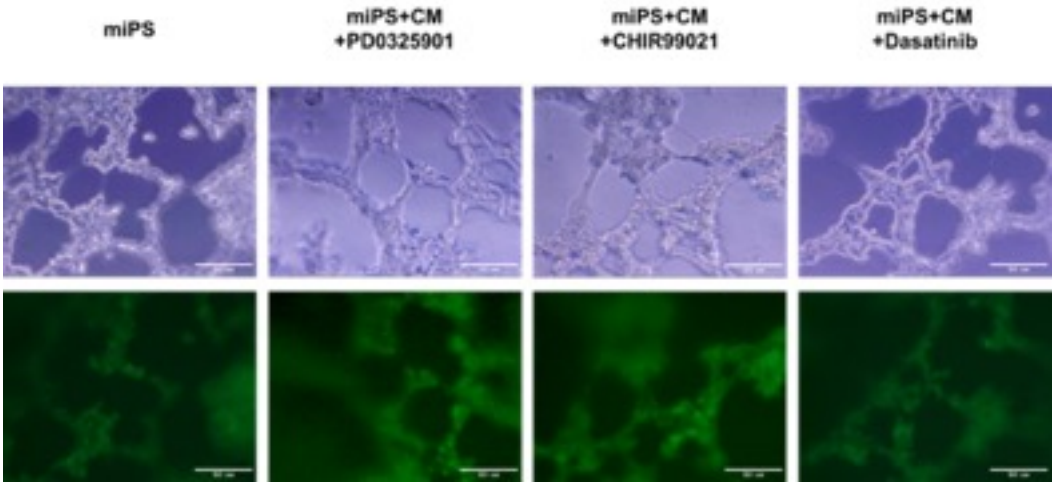

Figure 3.2. Tube formation assays in miPSCs and other three converted cells after 20 hours of culture with on Matrigel. These cells showed high potential of tube formation.

3.2.3 Tumorigenicity of GFP positive miPSCs after 1-week treatment

Considering the rise of self-renewal capacity of these cells and the results from our previous study, we investigated whether these compounds were effective in promoting the conversion from miPSCs into CSCs. To evaluate the tumorigenicity of these cells, 1×10^6 of these cells were subcutaneously transplanted into Balb/c nude mice and the tumor formation were excited for 6 weeks (Fig. 3.3A). Tumors formed at 6-week were excised (Fig. 3.3B) and subjected to histological and immuno-histochemical analysis (Fig. 3.3). As previously reported (16), miPSCs formed a teratoma phenotype with various normal germ layers, including the squamous epithelium, so called keratinized ball, skeletal muscle, cartilage and benign glandular epithelium (Fig. 3.4A). Tumors derived from miPSCs treated with PD0325901, CHIR99021 and Dasatinib formed malignant tumors, sections of which demonstrated poorly differentiated phenotype, high nuclear to cytoplasmic ratio, severe nuclear atypia and multiple pathological mitotic figures (Fig. 3.4B-D). They also exhibited multiple abnormal glands, trabecular patterns, necrosis in the glandular cavity, and large zones of necrosis in the mesenchymal tissue. Immuno-histochemical analysis demonstrated that the staining with Ki-67 antibody was highly proliferative, supporting the rapid tumor growth. The expression of CK and Sox2 indicated phenotypes of poor differentiation (Fig. 3.4E). Hence, the development of malignant tumor was confirmed by the GFP positive miPSCs treated with the inhibitors for 1-week (Tab. 3.1).

Table 3.1 Summary of tumorigenic potential of miPSCs treated in various conditions.

Supplement	Conditioned medium	Cell number	Tumor formation	Histologic examination
LIF (1000U/mL)	-	$1x10^6$	3/3	Benign teratoma
-	+	$1x10^6$	0/3	-
Mastinib (6.25 μM)	+	$1x10^6$	0/3	-
PD0325901 (5 μM)	+	$1x10^6$	3/3	Malignant tumor, adenocarcinoma
CHIR99021 (2.5 μM)	+	$1x10^6$	3/3	Malignant tumor, adenocarcinoma
Rabastinib (2.5 μM)	+	$1x10^6$	0/3	-
ALK5 Inhibitor (10 μM)	+	$1x10^6$	0/3	-
Dasatinib (1.25 μM)	+	$1x10^6$	3/3	Malignant tumor, adenocarcinoma
Imatinib (2.5 μM)	+	$1x10^6$	0/3	-
Ponatinib (0.625 μM)	+	$1x10^6$	0/3	-

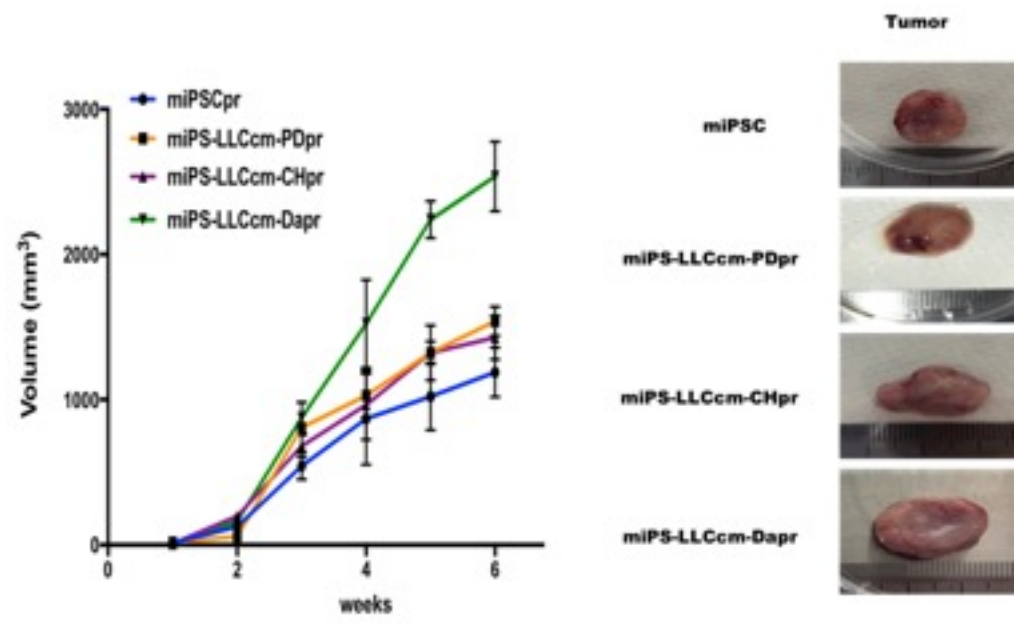

Figure 3.3 Tumorigenicity of CSCs converted from miPSCs treated with chemical compounds.

(A) The size of tumors growing in 6 weeks. (B) Generation of tumors after subcutaneously transplanted miPSCs and the 1-week of converted cells.

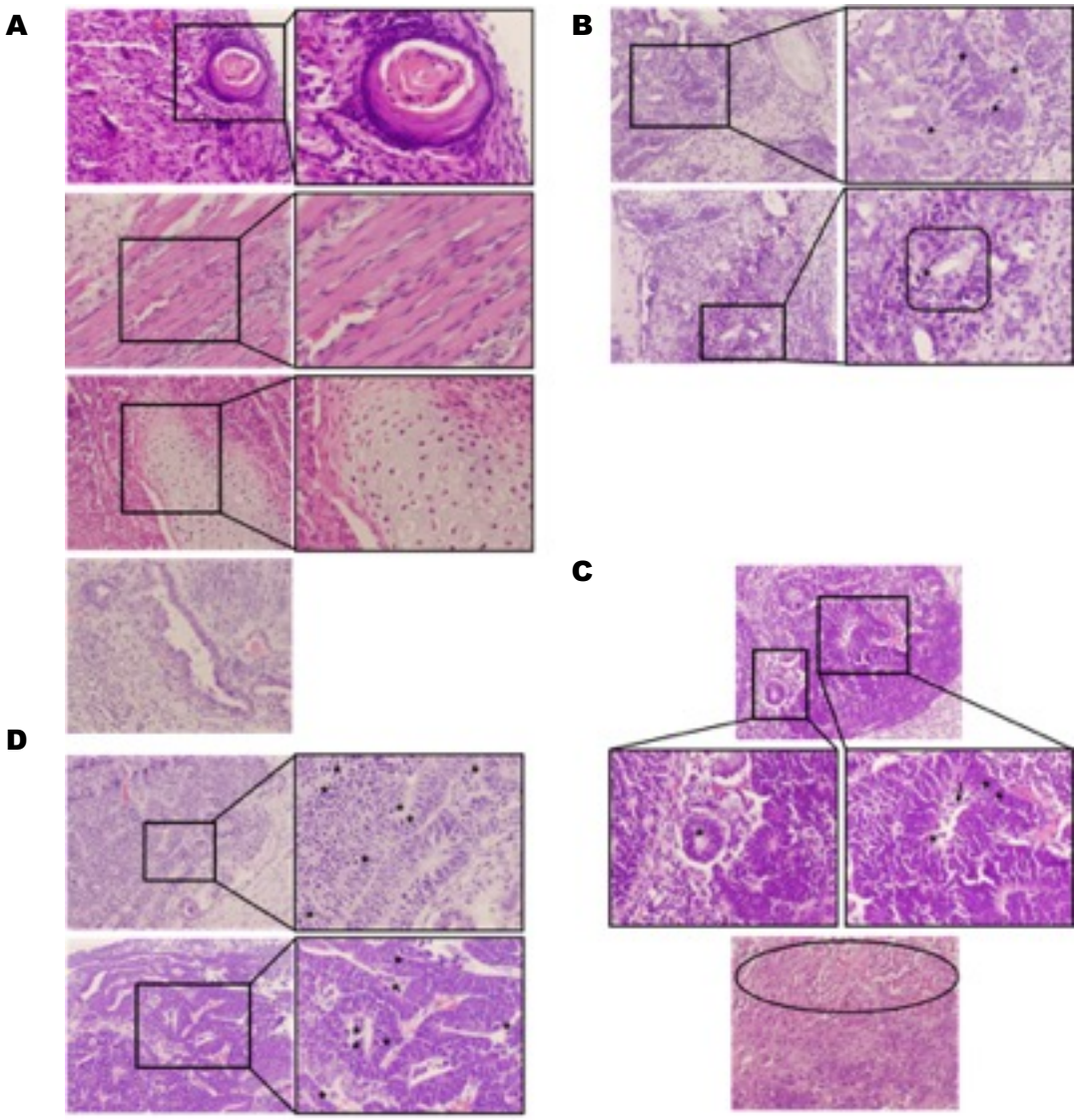
A
B
C
D

E

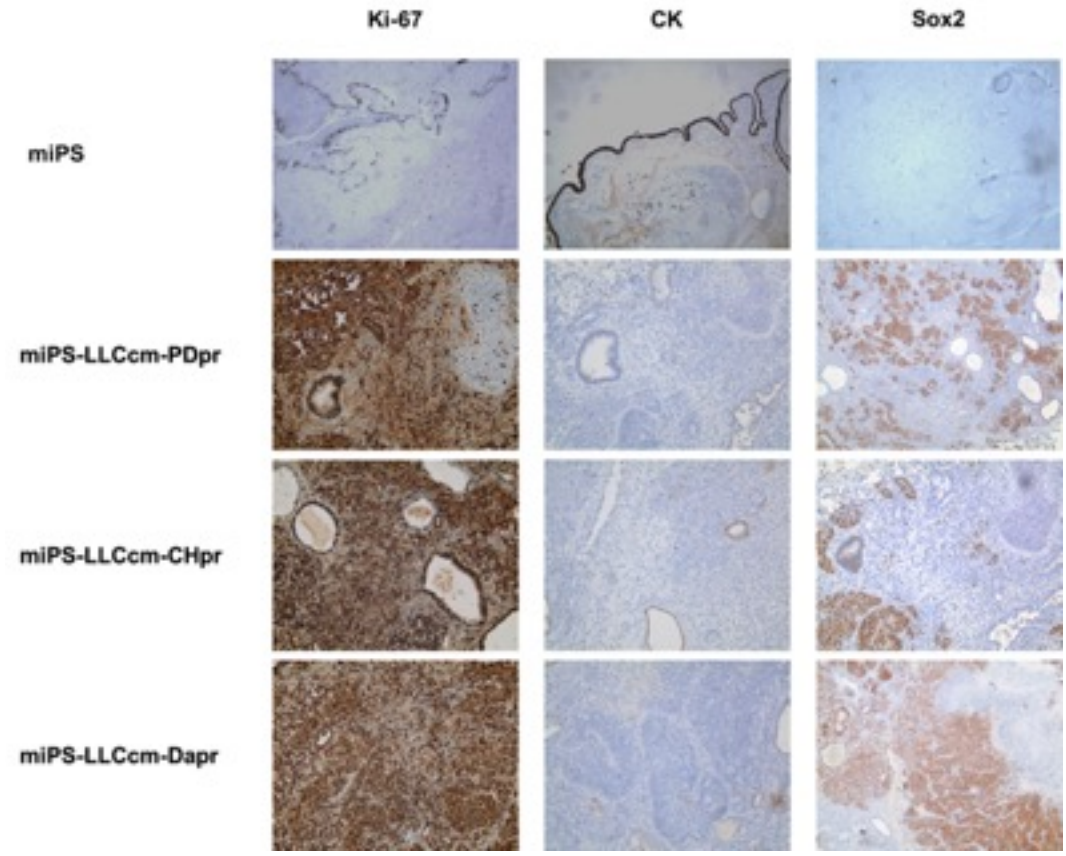

Figure 3.4 Histopathological observation of the tumors formed by the CSCs. (A) Benign teratoma fromed by miPSCs transplanted s.c. Normal tissue types derived from three germ layer, including squamous epithelium (Keratinized ball), skeletal muscle, cartilage and benign glandular epithelium are observed. Sections from the tumors formed by miPS-LLCcm-PD (B), miPS-LLCcm-CH (C) and miPS-LLCcm-Da (D) cells transplanted sc. Malignant structures are observed in glandular cavities (square，bottom right in B) composed of multiple abnormal glands, which are crowded back to back exhibiting high nuclear to cytoplasmic ratio, severe nuclear atypia and multiple pathological mitotic figures (asterisks in B, C, D). Abnormal glands, inside of glandular cavity has necrosis (arrow in C), and large

area necrosis (oval in C). Original magnification was 20X and 40X (A, B, C， D). (E) Immunohistochemical analysis showed malignancies with highly proliferative areas strongly stained for Ki-67 and poorly differentiated areas, poorly stained for CK and strongly for Sox2 in the tumor formed by miPS-LLCcm-PD, miPS-LLCcm-CH and miPS-LLCcm-Da when compared with the benign teratoma formed by miPSCs.

3.2.4 Self-renewal capacity of primary cells derived from tumors

To further evaluate the properties of primary tumors, the primary cells were cultured from the tumors developed in the previous section. The adhesive culture of the primary cells showed positive for GFP, indicating that they were originated from the miPSCs (Fig. 3.5A). In suspension culture, these cells were able to form spheroids indicating self-renewal capacity, and all spheroid-forming cells were expressing GFP (Fig. 3.5B). The expression level of *Oct3/4, Sox2, Nanog*, *Klf4* and *c-Myc* were observed in these cells using rt-qPCR (Fig. 3.5 C). *Oct3/4, Sox2, Nanog* and *Klf4* were found to be upregulated when compared with miPSCs. These results indicated that these cells possessed the self-renewal capacity.

A

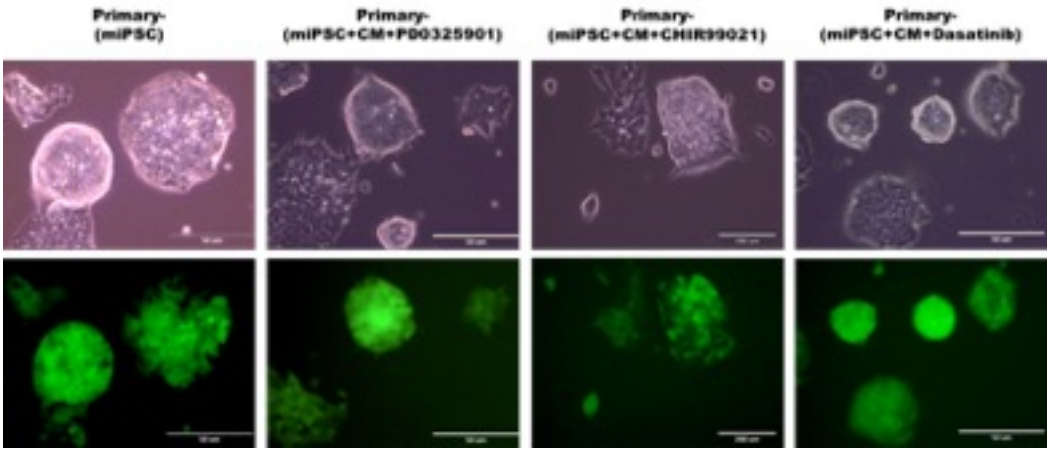
Primary-
(miPSC)
Primary-
(miPSC+CM+PD0325901)
Primary-
(miPSC+CM+CHIR99021)
Primary-
(miPSC+CM+Dasatinib)

B

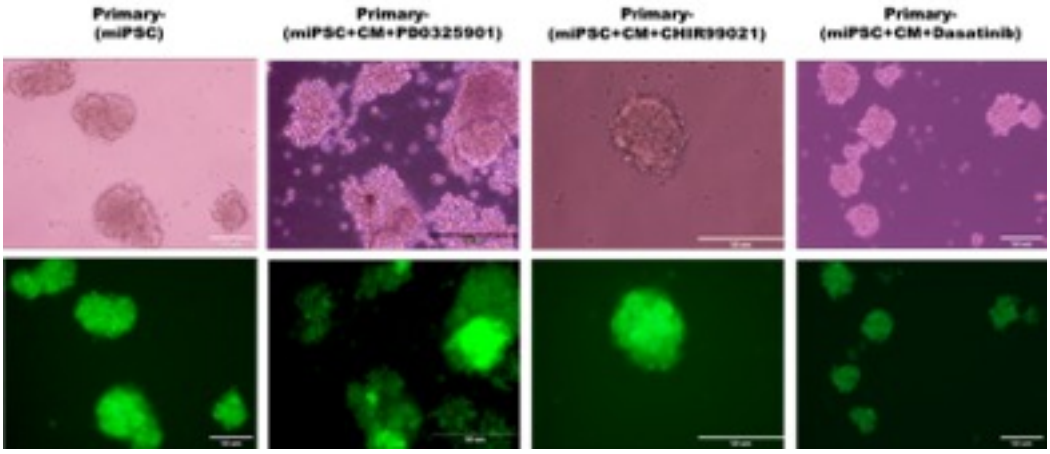
Primary-
(miPSC)
Primary-
(miPSC+CM+PD0325901)
Primary-
(miPSC+CM+CHIR99021)
Primary-
(miPSC+CM+Dasatinib)

C

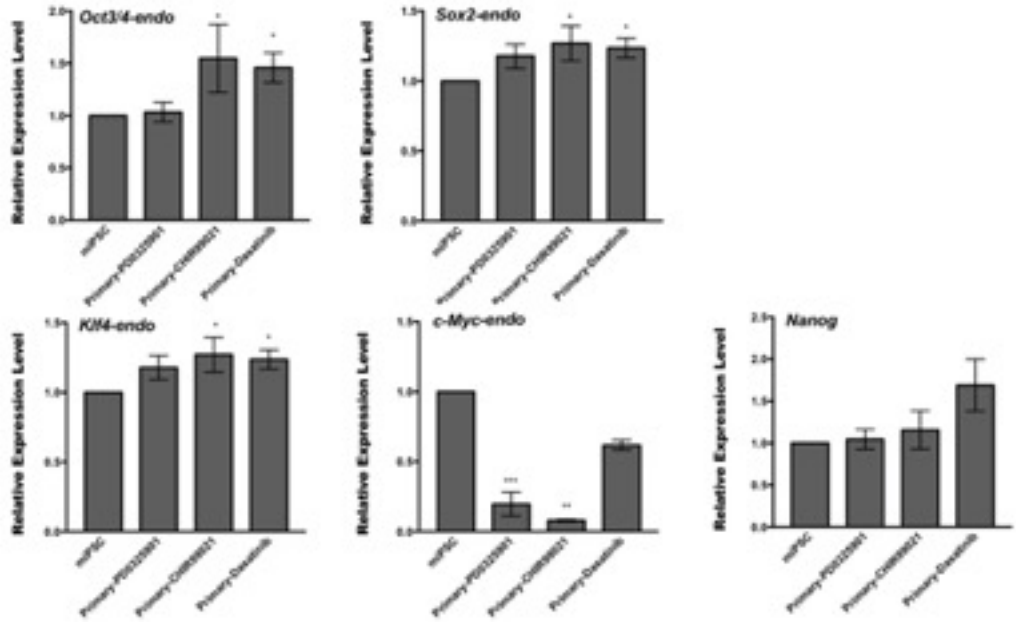

Figure 3.5 Primary culture cells possess self-renewal capacity.

(A and B) Primary cells in adherent culture and sphere formation in suspension culture with the expression of GFP. (C) rt-qPCR analysis of stemness markers in primary tumor cells. The data were analyzed using ordinary one-way ANOVA multiple comparisons and presented as the mean ± standard deviation ****P<0.0001, ***P<0.001, **P<0.01, *P<0.05.

3.2.5 Signaling inhibitors accelerated the conversion of miPSCs into CSCs activating the PI3K-AKT pathway

We labelled the primary cultured cells, obtained from the malignant tumors developed by transplanting miPSCs treated with each PD0325901, CHIR99021 and Dasatinib as miPS-LLCcm-PDpr, miPS-LLCcm-CHpr, miPS-LLCcm-Dapr, respectively. The signaling pathways of Ras-Raf-MEK-ERK, Abl, Src, c-Kit, Wnt-GSK3 and PI3K-Akt-mTOR are considered typically important in cancer cell growth and survival (17-19). Our results demonstrated that the inhibition of the pathways, expect PI3K, was effective in enhancing the induction of the CSCs. On the other hand, PI3K inhibitors did not enhance the induction of CSCs (Table S2). Furthermore, in our previous study, we reported that PI3K-Akt signaling pathway was up-regulated in the CSCs developed from miPSCs (20). Therefore, we evaluated the expression of PI3Ks in the CSCs, developed from miPSCs, in the presence of PD0325901, CHIR99021 and Dasatinib. Simultaneously, the expression of PTEN, which is considered to be antagonized by PI3K through the dephosphorylation of PIP_3 (21), was evaluated. We assessed the expression of *Pik3ca*, *Pik3cb*, *Pik3cg*, *Pik3r1*, *Pik3r5*, *Pik3r6* and *PTEN* using rt-qPCR in the primary cultured cells (Fig. 3.6 A). In the comparison to the miPSCs, *Pik3ca*, *Pik3cb*, *Pik3r1* and *Pik3r5* showed significantly high expression in the miPS-LLCcm-PDpr, miPS-LLCcm-CHpr and miPS-LLCcm-Dapr cells while *PTEN* showed low and *Pik3cg* and *Pik3r6* no expression. We assessed the phosphorylation of AKT by western blotting (Fig. 3.6B). We found AKT was constitutively activated in miPS-LLCcm-PDpr, miPS-LLCcm-CHpr, miPS-LLCcm-Dapr cells.

We then confirmed the expression of AKT1, AKT2 and mTOR using rt-qPCR (Fig. 3.6C). These findings are consistent with the enhanced PI3K-AKT signaling pathway enhanced in CSCs, as demonstrated in our previous study (20).

A

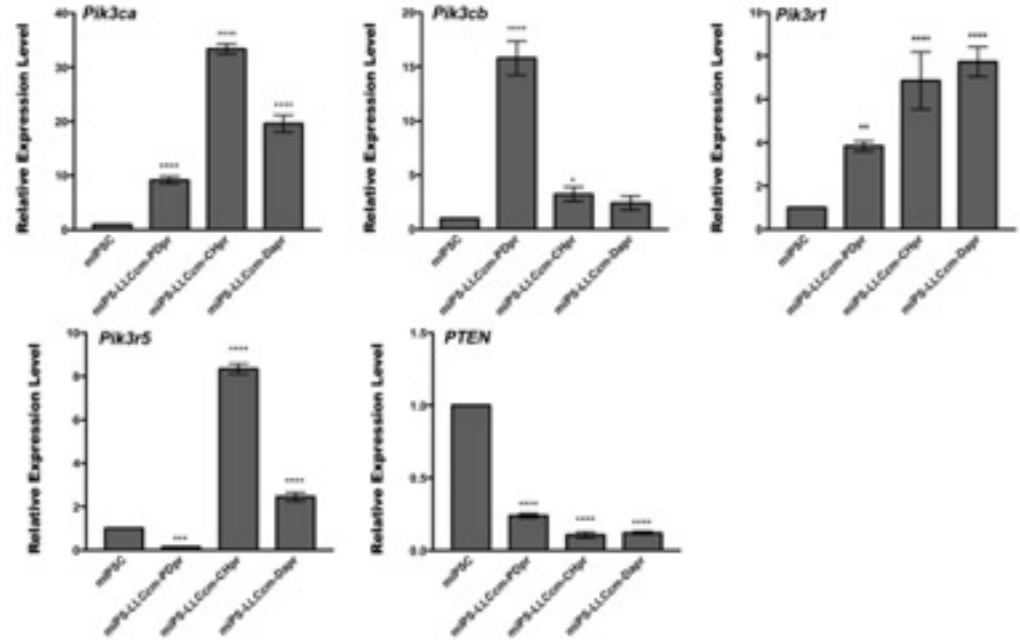
Pik3ca
Pik3cb
Pik3r1
Pik3r5
PTEN
Relative Expression Level
miPSC
miPS-LLCcm-PDpr
miPS-LLCcm-CHpr
miPS-LLCcm-Dapr

B

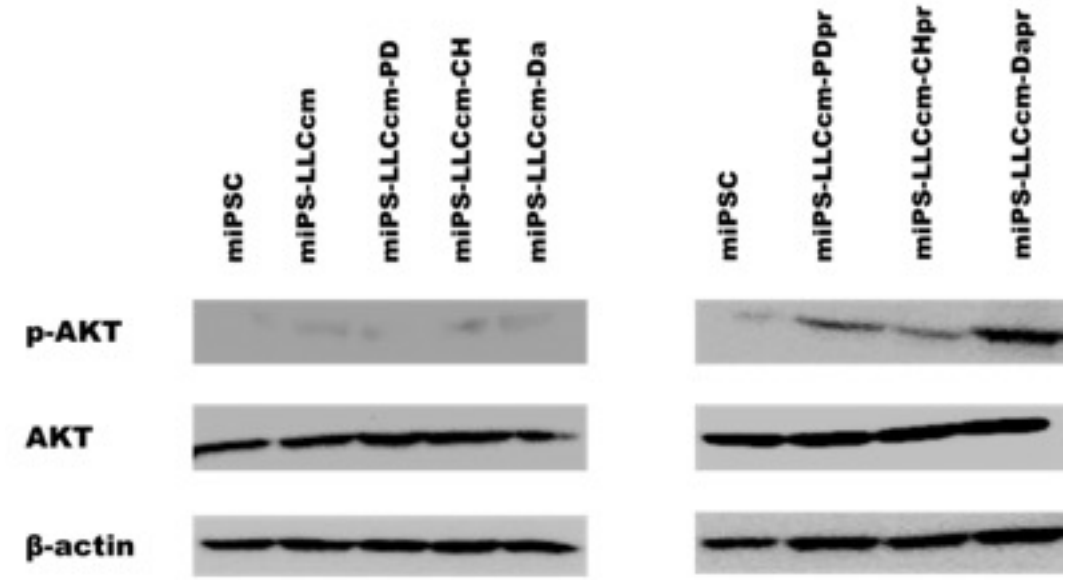
miPSC
miPS-LLCcm
miPS-LLCcm-PD
miPS-LLCcm-CH
miPS-LLCcm-Da
miPSC
miPS-LLCcm-PDpr
miPS-LLCcm-CHpr
miPS-LLCcm-Dapr
p-AKT
AKT
β-actin

C

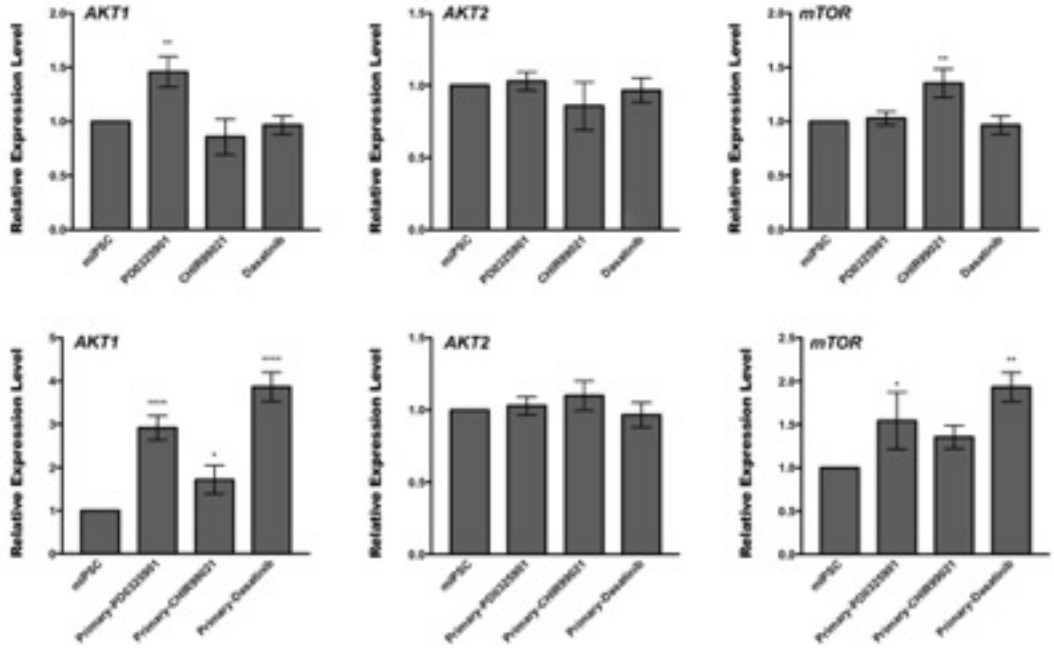

Figure 3.6 PI3K signaling pathway was activated in primary culture cells.

(A) rt-qPCR analysis of *Pik3ca*, *Pik3cb*, *Pik3r1*, *Pik3r5* and *PTEN* expression. (B) Immunoblotting analysis the AKT expression and phosphorylation. (C) rt-qPCR analysis of AKT1, AKT2 and mTOR.

3.3 Discussion

Our previous study demonstrated that the CM from cancer cell lines could provide a tumor microenvironment for conversion of miPSCs to CSCs (11-13). The tumor microenvironment (TME) plays an indispensable role in the development and progression of cancer. The stromal compartment of the TME comprises a variety of cell types, including endothelial cells, fibroblasts, and immune cells, each possessing distinct yet complementary functions that support the tumor architecture and maintenance. The specific tumor microenvironment can promote the occurrence of metastasis by affecting the proliferation of tumor cells, regulating the expression level of metastasis-associated genes, inducing angiogenesis, and promoting the degradation of the extracellular matrix (22). Recently we have found the overexpression of *pik3r5* and *pik3cg*, which are the components of class IB PI3 kinase, in CSCs derived from miPSCs cultured in the presence of CM (20). Although the miPS-LLCcm-PD, miPS-LLCcm-CH, miPS-LLCcm-Da cells are the resulted from the a 1-week treatment, we postulated that the PI3K/AKT pathway may be activated, as reported in our previous work. The western blotting analysis (Fig. 6B) detected a significant amount of immune reactive PI3K and phosphorylated AKT were detected in all the converted CSCs and the primary cultures derived from transplanted tumors. In accordance with the results obtained, we further investigated the expression levels of each moiety of PI3K, namely *Pik3ca*, *Pik3cb*, *Pik3cg*, *Pik3r1*, *Pik3r5* and *Pik3r6*. As the results, we found the overexpression of *Pik3ca*, *Pik3cb, Pik3r1* and *Pik3r5* as the candidates for the further investigation. *Pik3r1*and *Pik3ca*/*Pik3cb* are the components of class IA

PI3K while *Pik3r5* is the moiety of class IB. The expression of *Pik3cg,* the half moiety of class IB for *Pik3r5*, was too low to be amplified by rt-qPCR, and hence class IB PI3K was not considered to be active. Moreover, the combination of *Pik3r1*and *Pik3ca* formed PI3K that is activated through tyrosine kinase receptors and *Pik3r1* and *Pik3cb* form PI3K that is activated by G Protein-Coupled Receptors (GPCRs). Therefore, in response to various ligand stimulation, PI3K/AKT signal contributes to a variety of processes that are critical in mediating several aspects of cellular function, including nutrient uptake, metabolic reactions, cell growth and survival. Several previous studies have demonstrated that PI3K and AKT are frequently hyperactivated in the majority of cancers (23, 24).

Stemness markers, *Oct3/4*, *Sox2*, *Klf4* and *c-Myc*, are considered to perform a dominant role in the maintenance and self-renewal of ESCs and iPSCs (14). The expression of these four factors in miPS-LLCcm-PD, miPS-LLCcm-CH, and miPS-LLCcm-Da cells was found to vary when compared to miPSCs but the *Nanog* expression both as an endogenous gene and as GFP expression appeared steadily up-regulated. Therefore, the undifferentiated state of these cells could be maintained. Masatinib and Dasatinib were known as tyrosine kinase inhibitors of c-Kit and ABL1 / BCR-ABL1, respectively. Interestingly, miPSCs treated with Masatinib was not indicated as an inducer of CSCs in this study. These results may imply the different functions of tyrosine kinases involve in the stages of cellular differentiation. As c-Kit is known as the Stem Cell Factor receptor, Masatinib could have inhibited the signaling pathway essential for the self-renewal. On the other hand, Dasatinib might inhibit the growth of certain cells at partially differentiated

stages, resulting in the enhancement of self-renewal of the undifferentiated cells. PD0325901 is well known as MEK1/2 inhibitor. MEK is a main downstream of tyrosine kinases from the Ras/Raf/MAP kinase cascade, and PD0325901 appeared to conceivably induce the conversion of miPSCs to CSCs, as did Dasatinib. CHIR99021 is an inhibitor of GSK-3β, which plays a role in the downstream of signaling of Wnt. As Wnt suppresses the function of GSK-3β, CHIR99021 should act as Wnt resulting in the activation of β-catenin-Lef/Tcf signaling, which is considered necessary to maintain CSCs (25-27). Ying et al. reported that the self-renewal potential of mouse ESCs was maintained in the presence of CHIR99021 and PD0325901 (28). In this context, down-modulation of GSK-3β could result in a crucial stage to maintain metabolic activity, biosynthetic capacity and overall viability resulting in the decrease of phospho-ERK through the attenuation of MEK1/2, which reversed, would support our results. Hence, these inhibitors appear to relatively activate the PI3K/AKT pathway.

Our study demonstrated that the three cellular signaling inhibitors accelerated the conversion of miPSCs into CSCs during 1-week treatment in the presence of a CM from LLC cells. In each case of treatment, the PI3K/AKT signaling pathway was reported to be activated. The genes responsible for PI3K were considered to form class IA and IB. This means that the CM from LLC contains the crucial factor(s), which could stimulate tyrosine kinase receptors and/or the GPCRs, responsible for the conversion resulting in the enhancement of PI3K/AKT signaling pathway. The mechanisms, by which PI3K regulates self-renewal and pluripotency, remain somewhat elusive. However, the contribution of PI3K/AKT signaling in

preserving the ability of iPSCs to self-renewal and differentiation is being delineated in recent studies (29, 30). Finally, this signaling pathway has been found crucial for CSC development as well as for embryonic and/or iPSCs development. Hishida et al suggested that PI3K promoted the retention of ES cell properties mainly through the inhibition of the two downstream pathways, the mitogen-activated protein kinases/extracellular signal-regulated kinase (MAPK/ERK) pathway and the GSK3 signaling pathway (31). Previous studies from several groups have demonstrated that certain AKT downstream factors such as *Oct3/4*, *Sox2* and *Nanog*, play an important role in self-renewal of ESCs and the early development of embryos (32-34). Meanwhile, these markers are also the targets of the AKT signaling pathway phosphorylating T^{235} in Oct4 to maintain stemness and inhibit differentiation of iPS cells (35). Thus, the enhanced conversion of the iPSCs into CSCs could be explained in as similar manner. An important factor to be considered is that the iPSCs derived from malignant cells differentiated in to cancer cell types of interest. Henceforth, the finding of our study will allow the possibility of a short evaluation time to identify the crucial factor(s) present in the tumor microenvironment.

References

1. Clevers H (2011). The cancer stem cell: premises, promises and challenges. *J Nat Med* **17**, 313-319.

2. Safa AR, Saadatzadeh MR, Cohen-Gadol AA, et al (2015). Glioblastoma stem cells (GSCs) epigenetic plasticity and interconvertsion between differentiated non-GSCs and GSCs. *J Genes Dis* **2**, 152-163.

3. Friedmann-Morvinski D (2014). Glioblastoma heterogeneity and cancer cell plasticity. *J Crit Rev Oncog* **19**, 327-336.

4. Engelman JA, Luo J, Cantley LC (2006). The evolution of phosphatidylinositol 3- kinases as regulators of growth and metabolism. *Nat Rev Genet* **7**, 606-19.

5. Lin J, Adam RM, Santiestevan E, Freeman MR (1999). The phosphatidylinositol 3-kinase pathway is a dominant growth factor-activated cell survival pathway in LNCaP human prostate carcinoma cells. *Cancer Res* **59**, 2891-2897.

6. Fry MJ (2001). Phosphoinositide 3-kinase signaling in breast cancer: how big a role might it play? *Breast Cancer Res* **3**, 304-312.

7. Lin X, Bohle AS, Dohrmann P, Leuschner I, Schulz A, Kremer B et al (2001). Overexpression of phosphatidylinositol 3-kinase in human lung cancer. *Langenbecks Arch Surg* **386**, 293-301.

8. Krasilnikov M, Adler V, Fuchs SY, Dong Z, Haimovitz-Friedman A, Herlyn M et al (1999). Contribution of phosphatidylinositol 3-kinase to radiation resistance in human melanoma cells. *Mol Carcinog* **24**, 64-69.

9. Martinez-Lorenzo MJ, Anel A, Monleon I, Sierra JJ, Pineiro A, Naval J et al (2000). Tyrosine phosphorylation of the p85 subunit of phosphatidylinositol 3-kinase correlates with high proliferation rates in sublines derived from the Jurkat leukemia. *Int J Biochem Cell Biol* **32**, 435-445.

10. Nicholson KM, Anderson NG (2002). The protein kinase B/Akt signaling pathway in human malignancy. *Cell Signal* **14**, 381-395.

11. Chen L, Kasai T, Li Y, Sugii Y, Jin G, Okada M, Vaidyanath A, Mizutani A, Satoh A, and Kudoh T, et al (2012). A model of cancer stem cells derived from mouse induced pluripotent stem cells. *PLoS One* **7**, e33544.

12. Calle AS, Nair N, Oo AKK, Prieto-Vila M, Koga M, Khayrani AC, Zahra MH, Hurley L, Vaidyanath A, and Seno A, et al (2016). A new PDAC mouse model originated from iPSCs-converted pancreatic cancer stem cells (CSCcm). *Am J Cancer Res* **6**, 2799-2815.

13. Nair N, Calle AS, Zahra MH, Prieto-Vila M, Oo AKK, Hurley L, Vaidyanath A, Seno A, Masuda J, and Iwasaki Y, et al (2017). A cancer stem cell model as the point of origin of cancer-associated fibroblasts in tumor microenvironment. *Sci Rep* **7**(1),6838.

14. Okita K, Ichisaka T and Yamanaka S (2007). Generation of germline-competent induced pluripotent stem cells. *Nature* **448**, 313.

15. Pastrana, E., Silva-Vargas, V. & Doetsch, F (2011). Eyes wide open: a critical review of sphere-formation as an assay for stem cells. *Cell stem cell* **8**, 486-498.

16. Takahashi K and Yamanaka S (2006). Induction of pluripotent stem cells from mouse embryonic and adult fibroblast cultures by defined factors. *Cell* **126**, 663-76.

17. Kitagishi Y, Kobayashi M, Kikuta K,Matsuda S (2012). Roles of PI3K /AKT /GSK3 /mTOR Pathway in Cell Signaling of Mental Illnesses. Depress Res Treat. 2012:752563.

18. Tenbaum S P, Paloma Ordóñez-Morán, Isabel Puig et al (2012). β-catenin confers resistance to PI3K and AKT inhibitors and subverts FOXO3a to promote metastasis in colon cancer. Nat Med. **8**(6):892-901.

19. Zhan T, Rindtorff N and Boutros M (2017).Wnt signaling in cancer. Oncogene. **36**(11): 1461-1473.

20. Oo AKK, Calle AS, Neha N, et al (2018). Regulation of PI 3-Kinases and the Activation of PI3K-Akt Signaling Pathway in Cancer Stem-Like Cells

Through DNA Hypomethylation Mediated by the Cancer Microenvironment. Translational Oncology **11**, 653-663.

21. Francesca M and Milo F (2014). Functions and regulation of the PTEN gene in colorectal cancer. Front Oncol. **3**: 326.

22. Madar, S., Goldstein, I. & Rotter, V (2013). Cancer associated fibroblasts–more than meets the eye. *Trends Mol. Med* **19**, 447-453.

23. Vanhaesebroeck, B, Guillermet-Guibert, J, Graupera M and Bilanges B (2010). The emerging mechanisms of isoform-specific PI3K signaling. *Nat. Rev. Mol. Cell Biol* **11**, 329-341.

24. Thorpe LM, Yuzugullu H. and Zhao J. J (2015). PI3K in cancer: divergent roles of isoforms, modes of activation and therapeutic targeting. *Nat. Rev. Cancer* **15**, 7-24.

25. Hishida T., Nakachi, Y., Mizuno Y. et al (2015). Functional Compensation Between Myc and PI3K Signaling Supports Self-Renewal of Embryonic Stem Cells. *Stem Cells* **33**, 713-725.

26. Golestaneh N., Beauchamp E., Fallen S. et al (2009). Wnt signaling promotes proliferation and stemness regulation of spermatogonia stem/progenitor cells. *Reproduction* **138**, 1470-1626.

27. Dravid, G., Zhao, H. E., Hammond, H. et al (2005). Defining the Role of Wnt/β-Catenin Signaling in the Survival, Proliferation, and Self-Renewal of Human Embryonic Stem Cells. *Stem Cells* **23**, 1489-1501.

28. Ying Q L, Wray J, Nichols J, et al (2008). The ground state of embryonic stem cell self-renewal (J). *Nature* **453**(7194), 519–523.

29. Paling, N. R. D., Wheadon, H., Bone, H. K. and Welham, M. J (2004). Regulation of embryonic stem cell self-renewal by phosphoinositide 3-kinase-dependent signaling. *J. Biol. Chem* **279**, 48063-48070.

30. Singh, A. M., Reynolds, D., Cliff, T., Ohtsuka, S., Mattheyses, A. L., Sun, Y., Menendez, L., Kulik, M. and Dalton, S (2012). Signaling network crosstalk in human pluripotent cells: a Smad2/3-regulated switch that controls the balance between self-renewal and differentiation. *Cell Stem Cell* **10**, 312-326.

31. Hishida, T., Nakachi, Y., Mizuno, Y., Katano, M., Okazaki, Y., Ema, M., Takahashi, S., Hirasaki, M., Suzuki, A., Ueda, A. et al (2015). Functional compensation between Myc and PI3K signaling supports self-renewal of embryonic stem cells. *Stem Cells* **33**, 713-725.

32. Chen J, Crawford R, Chen C, Xiao Y (2013). The key regulatory roles of the PI3K/Akt signaling pathway in the functionalities of mesenchymal stem cells and applications in tissue regeneration. *Tissue Eng Part B Rev* **19**(6), 516-28.

33. Kolf CM, Cho E, Tuan RS (2007). Mesenchymal stromal cells. Biology of adult mesenchymal stem cells: regulation of niche, self-renewal and differentiation. *Arthritis Res Ther* **9**(1), 204.

34. Liu TM, Wu YN, Guo XM, Hui JH, Lee EH, Lim B (2009). Effects of ectopic Nanog and Oct4 overexpression on mesenchymal stem cells. *Stem Cells* **18**(7), 1013-22.

35. Klemm JD, Rould MA, Aurora R (1994). Crystal structure of the Oct-1 POU domain bound to an octamer site: DNA recognition with tethered DNA-binding modules. *Cell* **77**(1), 21-32.

CHAPTER 4

Upregulated Ccl20 and Ccr6 in cancer stem cells converted from mouse iPS cells

Abstract

Previous studies by our group have demonstrated the establishment of the model of cancer stem cells (CSCs) converting mouse iPS cells (miPSCs) into CSCs by treating the miPSCs with a conditioned medium (CM) of Lewis Lung Carcinoma (LLC) cells, with or without the non-mutagenic chemical compounds. CSCs converted from miPSCs developed highly malignant adenocarcinoma when subcutaneously transplanted into the nude mice. We evaluated the gene expression in the resultant CSCs comparing that in miPSCs by microarray analysis. As the result, the expression of chemokine (C-C motif) ligand 20 (Ccl20) was found upregulated in the presence of CM supplemented with PD0325901. Then we assessed the expression of C-C chemokine receptor type 6 (Ccr6), which was considered to be stimulated by Ccl20, using rt-qPCR. Then the expression of Ccr6 was also found upregulated. Interestingly, IL17A expression was also observed only in the CSCs from the primary tumor implying the effect of the tumor microenvironment. Moreover, significantly high level of CCR6 was detected by flow cytometric analysis and western blotting. These results suggest that a model of CSCs with Ccl20-Ccr6 autocrine loop was obtained as the result of the conversion of miPSCs. This CSC should be a good model to study targeting CCR6 as a G protein-coupled receptor (GPCR).

4.1 Introduction

CSCs has been identified as a subpopulation of stem-like cells within tumors exhibiting characteristics of both stem cells and cancer cells. CSCs are characterized by the abilities of self-renewal, differentiation in vitro and tumorigenesis in vivo (1). CSCs are nowadays generally considered to represent a unique population of cancer tissues that are tumorigenic and resistant to most chemotherapeutic agents and radiation therapy supporting cancer progression and recurrence.

The molecular and cellular mechanisms of cancer progression are now significantly being studied due to the finding of CSCs. Chronic inflammation is considered one of the reasons essential for cancer initiation and progression providing tumor microenvironment. Chemokines are known to play a prominent role in inflammation and spreading of cancer. Therefore, chemokines and their cognate receptors should be important factors involved in wound healing and angiogenesis. The ligands and their receptors are generally expressed in various cells in response to inflammation to recover homeostasis from imbalanced situation (2).

Previously, our group has demonstrated the development of CSCs from miPSCs treating with the CM derived various cancer cell lines (3-5). The conditioned medium was supposed to be enriched with various factors related with tumor microenvironment including inflammatory cytokines, chemokines and

growth factors. One of our recent findings in the CSCs was an enhanced expression of PI3 kinase, which was considered to be responsible for the activation of GPCRs (6).

On the other hand, chemokine CCL20 is considered a sole known ligand specific to CCR6, one of the GPCRs. Their interaction has been confirmed in B and T cells as well as dendritic cells (DCs) (7-9). The interaction of CCL20 and CCR6 plays a key role in lung immunity while CCR6 has recently been reported to promote the carcinogenesis of non-small-cell-lung cancer (NSCLC) in CCR6/CCL20/IL17 axis (10-14).

IL17, a pro-inflammatory cytokine, stimulates several signaling cascades inducing chemokines including CCL20 as well. A recent study in a mouse model of rheumatoid arthritis has shown that Th17 cells express both CCR6 and CCL20, suggesting CCL20 induced recruitment of Th17 cells to the inflamed joints (15). Responding to IL17 in an autocrine manner, Th17 cells differentiate to produce CCL20 in vitro and in vivo (16,17). Since we found our CSCs overexpress CCL20 by microarray analysis, the presence of CCR6/CCL20/IL17 axis in the CSCs is evaluated in the current study.

4.2 Results and Discussion

4.2.1 The effect of chemical compounds during the conversion of miPSCs into CSCs

Previously, we found miPSCs converted into CSCs, exhibiting self-renewal, differentiation potential and tumorigenesis, in the presence of CM of cancer derived cell lines in 4 weeks (3-5). We employed miPSCs expressing a gene encoding green fluorescent protein (GFP) under the control of Nanog promoter (18) to distinguish the undifferentiated/differentiated condition of the cells. In the miPSCs, the GFP fluorescence is kept on during the undifferentiated state, while GFP fluorescence is turned off if the miPSCs normally differentiate in the absence of leukemia inhibitory factor (LIF). Applying this procedure, we assessed the risk of non-mutagenic chemical compounds to accelerate the conversion, which was taken as cancer initiation, in this study. Most of the compounds assessed were the inhibitors of cytoplasmic signaling pathways. As the results, the expression of GFP fluorescence were obviously maintained after 1 week when miPSCs were cultured with PD0325901 in the presence of CM from LLC cells (Fig.4.1). In contrast, All-Trans Retinoic Acid (ATRA) significantly accelerated diminishing GFP fluorescence indicating the cells differentiated. In our recent study, we have demonstrated that three compounds, PD0325901, CHIR99021 and Dasatinib, out of 110 could accelerate the conversion of miPSCs into CSCs, and the expression of GFP fluorescence were maintained (6). PD0325901 is known as an inhibitor of MEK, and MEK is a main downstream of tyrosine kinases from Ras/Raf/MAP

kinase cascade. Since Dasatinib is known as the tyrosine kinase inhibitor of src, bcl and c-kit, PD0325901 and Dasatinib appeared to have similar role in converting miPSCs into CSCs. When PD0325901 combined with CHIR99021 together the self-renewal potential of mouse ESCs was maintained while CHIR99021 was an inhibitor of GSK-3β (19). In this context, the functions of three inhibitors might closely be related one another to enhance the expression of GFP fluorescence and maintain the stemness resulting in the conversion from miPSCs into CSCs.

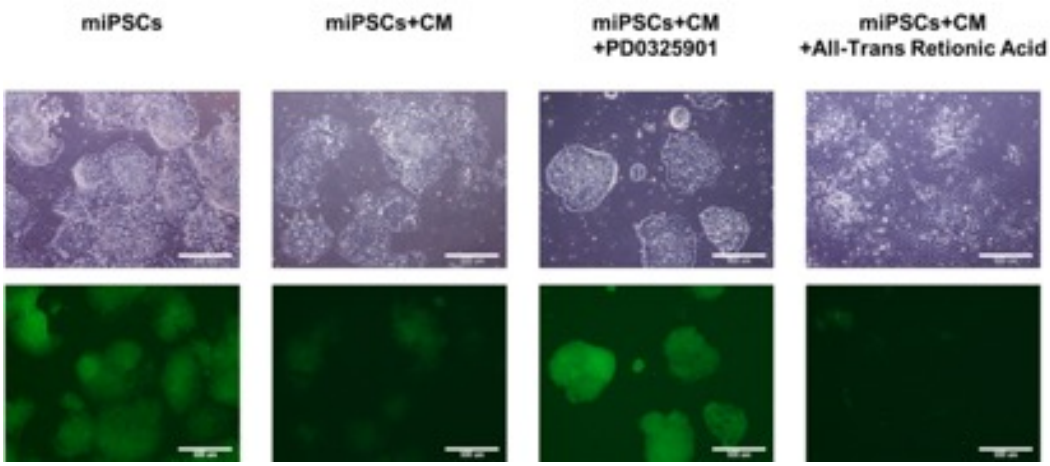

Fig. 4.1. Representative images of the conversion from miPSCs into CSCs. Cells were cultured with media containing CM and positive (PD0325901) / negative (All-Trans Retinoic Acid) chemical compound, colonies were observed for the GFP expression after treatment one week.

4.4.2 Gene expression difference during the conversion into CSCs treated with MEK inhibitor

PD0325901 kept the expression of GFP fluorescence high in the treated cells. In our previous study, we demonstrated that the PD0325901promoted the conversion from miPSCs into CSCs (6). Herein we analyzed the difference of gene expression between the cells treated with PD0325901and ATRA by microarray followed by gene clustering analysis with self-organizing map (SOM) (20-22). First of all, miPSC and miPSC treated with CM was compared to reveal the genes which is related to CSC conversion. There were 507 upregulated and 447 downregulated genes (Fig. 4.2). PD0325901 should have effects on them during the CSC conversion. These gene expressions were analyzed again and found 389 genes, whose expression was significantly upregulated or downregulated by PD0325901 when compared with those in miPSCs treated with ATRA (Table 4.1). Then, SOM was used to find an ideally expressed gene, which was named as an ideal probe (IP) and was not expressed in miPSC treated with CM or with CM and ATRA but highly expressed in miPSCs treated with CM and PD0325901. The distance from the IP was sorted from the shortest to the longest and the shortest genes are shown in Fig.4.2C. The genes in the short distance to IP should have larger effect by PD0325901. From this point of view, CCL20 could be the candidate to be analyzed for the relationship with CSCs and PD0325901.

Table 4.1. Distance from ideal probe and heat map for their expression levels.

From IP	Agilent ID	a b c	Systematic Name	David ID	Name
0.000	A_51_P323770		NM_183271	68221	WAP four-disulfide core domain 15A (Wfdc15a)
0.404	A_52_P455370		NM_175628	232345	alpha-2-macroglobulin (A2m)
0.406	A_66_P101506		AK077242		
0.453	A_55_P2728797		AK018940	68208	RIKEN cDNA 1700039O17 gene (1700039O17Rik)
0.453	A_55_P2168383		NM_028901	74376	myosin XVIllb (Myo18b)
0.460	A_52_P467488		NM_029529	76157	solute carrier family 35, member D3 (Slc35d3)
0.700	A_55_P2731446		XM_011245278	101055806	predicted gene 10378 (Gm10378)
1.281	A_51_P408595		NM_016960	20297	chemokine (C-C motif) ligand 20 (Ccl20)
1.551	A_51_P315391		NM_138628	378431	taxilin beta (Txlnb)
1.600	A_51_P471659		NM_145684	11685	arachidonate lipoxygenase, epidermal (Alox12e)
1.656	A_55_P2900459		XR_868020		
1.675	A_55_P1955871		NM_175290	97895	NLR family, pyrin domain containing 4F (Nlrp4f)
1.675	A_51_P208145		NM_021882	20431	premelanosome protein (Pmel)
1.767	A_55_P2153021		NM_011652	22138	titin (Ttn)
1.767	A_52_P306007		NM_024271	76413	RIKEN cDNA 1700016D06 gene (1700016D06Rik)
1.858	A_51_P291227		NM_001005508	226652	Rho GTPase activating protein 30 (Arhgap30)
1.858	A_55_P2031999		NM_145448	217830	RIKEN cDNA 9030617O03 gene (9030617O03Rik)

* The maximum distance from IP was 4.222, and genes whose distance is less than 2 is shown in this list.

(a: miPSC+CM, b: miPSC+CM+PD0325901, c: miPSC+CM+ARTA)

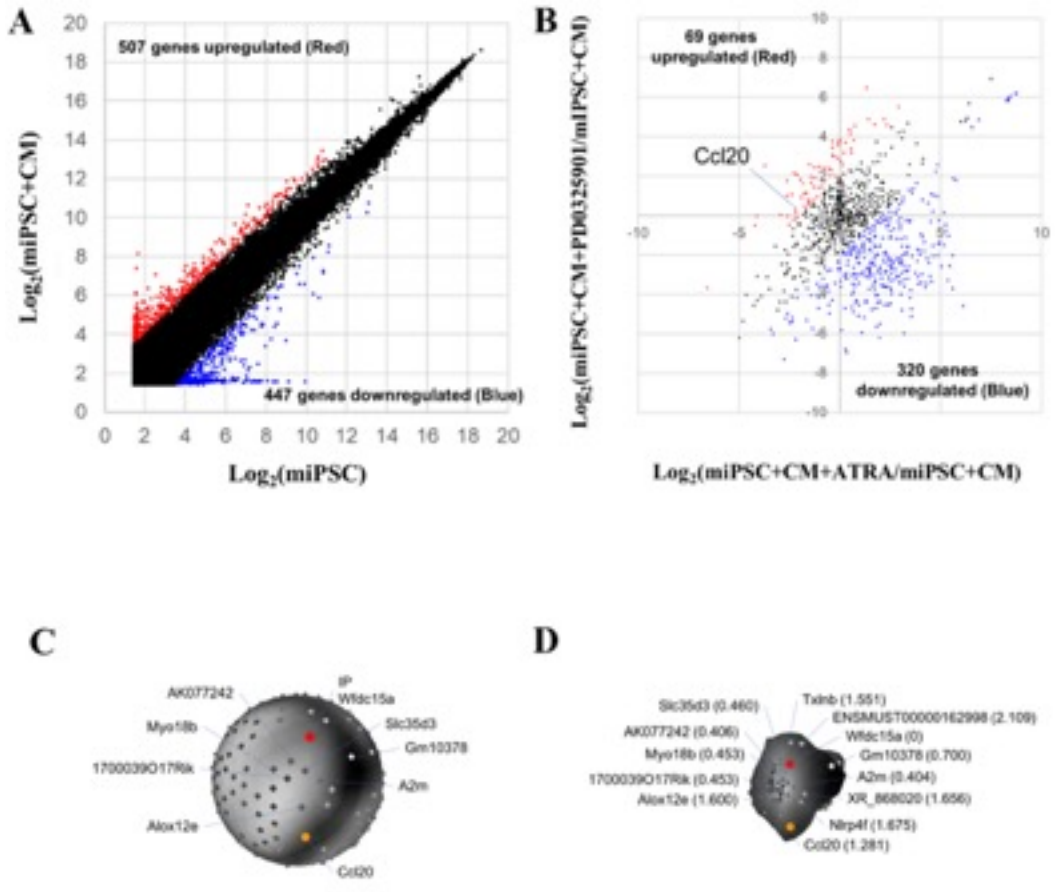

Fig. 4.2. Comparisons of gene expression among miPSC and 1 week converted cells. Microarray was performed on original miPSC and converted cells and their expression value were compared in binary logarithm among. (A) miPSC and miPSC+CM, and (B) miPSC+CM+All trans retinoic acid (ATRA) and miPSC+CM+PD0325901. (C and D) Glyph Analysis Setting > Dent rate = 1.

4.2.3 Expression of Il17A, Ccl20 and Ccr6 in converted cells and primary cultured cells were upregulated

Considering the results of SOM analysis, we evaluated the expression of Ccl20, which was up-regulated the distinctive gene expression profiles of miPSCs treated with PD0325901 in the presence of CM because CCL20 is significantly associate with inflammatory events, which could be related with the initiation of cancers. Multiple studies have now reported that IL17 could induce CCL20 production and CCR6, which might be leading to PI3K activation, as the unique receptor to CCL20 (23-25). Accordingly, we though Ccl20 expression might account for the presence of both Il17A and Ccr6 expression in CSCs converted from miPSCs. We further analyzed the expression of Il17A, Ccr6 and Ccl20 in miPSCs treated with PD0325901, CHIR99021 and Dasatinib by RT-qPCR. The expression level of Il17A, Ccr6 and Ccl20 were found to be upregulated during the 7 days of treatment (Fig.4.3A). Our previous work demonstrated that miPSCs treated with the three compounds exhibited tumorigenicity when subcutaneously transplanted into Balb/c nude mice (6). Meanwhile, we evaluated the expression of Il17A, Ccr6 and Ccl20 in the primary cells (Fig.4.3B). As the result, the significantly high expression of Ccr6 was found in the primary cells. Recent studies have reported that IL17A, of which expression was driving by TGF-β and IL-6, induced Ccl20 expression via the transcription factor STAT3 resulting in promoting tumor progression and metastasis by upregulating the expression of the genes were involved in anti-apoptotic, growth factors and angiogenesis (26,27).

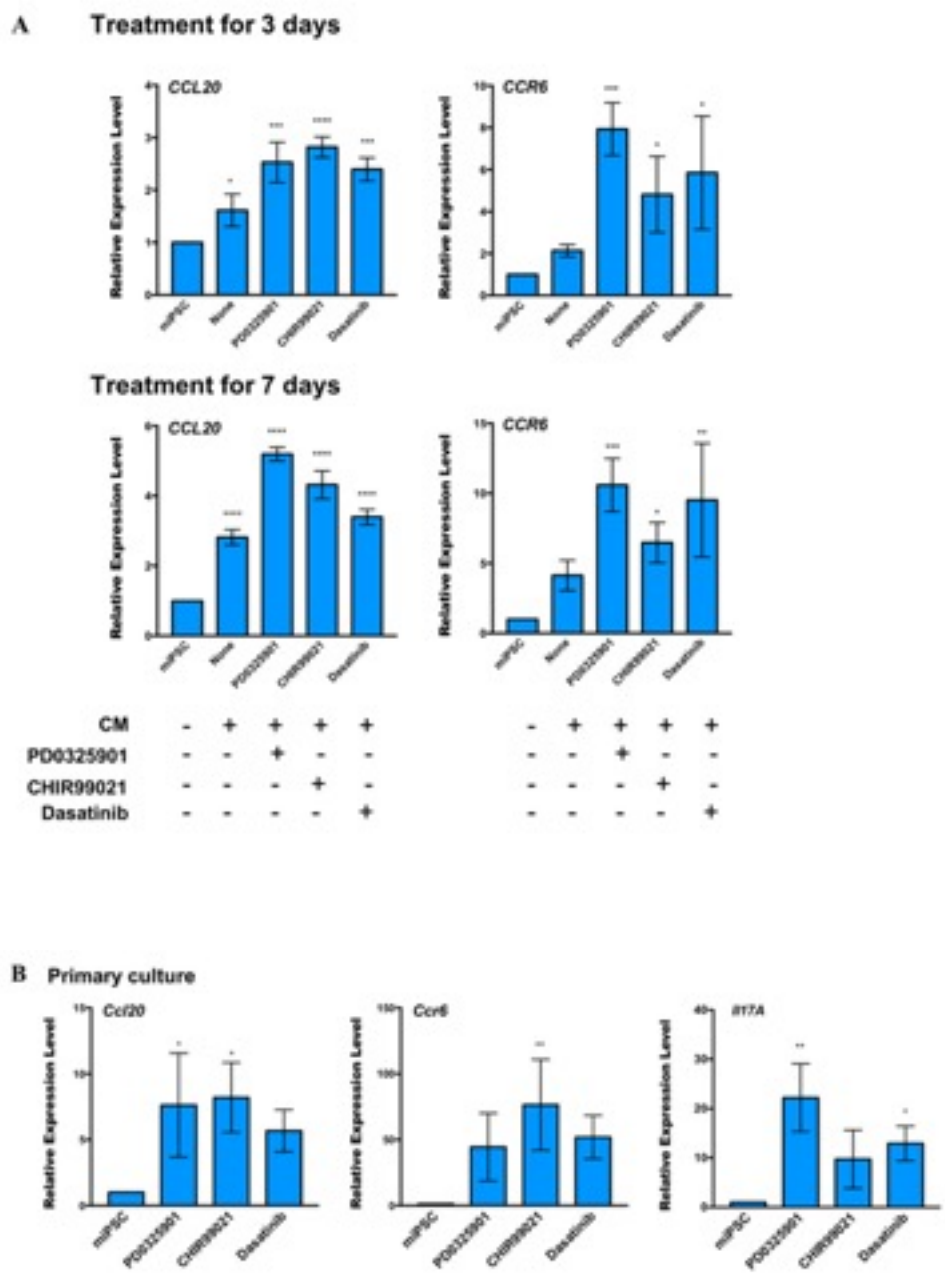

Fig. 4.3. Expression of Il17A, Ccl20 and Ccr6 in converted cells and primary cultured cells. (A) RT-qPCR analysis of Ccr6 and Ccl20 in the converted cells. (B) RT-qPCR analysis of Il17A, Ccr6 and Ccl20 in the primary cells from tumors. The data were analyzed using ordinary one-way ANOVA multiple comparisons and presented as the mean ± standard deviation ****P<0.0001, ***P<0.001, **P<0.01, *P<0.05.

4.2.4 The inhibitors enhanced the expression of Ccr6

Upregulation of Ccr6 expression was essentially related with organ orientation and significantly related with the metastasis of lung cancer (28-30). We further evaluated the expression of CCR6 by flow cytometry and western blot. In flow cytometry, the CCR6-postive population in the presence of CM was found 41.1%, 21.7% and 31.6% in the cells when treated with PD0325901, CHIR99021 and Dasatinib, respectively while 27.4% in miPSCs. CCR6-postive population was 3.9% of miPSCs in the absence of CM (Fig.4.4A). In the primary cells from the tumors, CCR6-postive population was significantly increased to 53.4%, 83.1% and 61.5% in primary-miPSCs+CM+PD0325901 cells, primary-miPSCs+CM+CHIR99021 cells and primary-miPSCs+CM+Dasatinib cells, respectively. CCR6-postive population was 10.6% of primary-miPSCs cells (Fig.4.4B). Furthermore, western blot analysis confirmed higher amount of CCR6 protein in the converted cells and primary cells than that in miPSCs (Fig.4.4C).

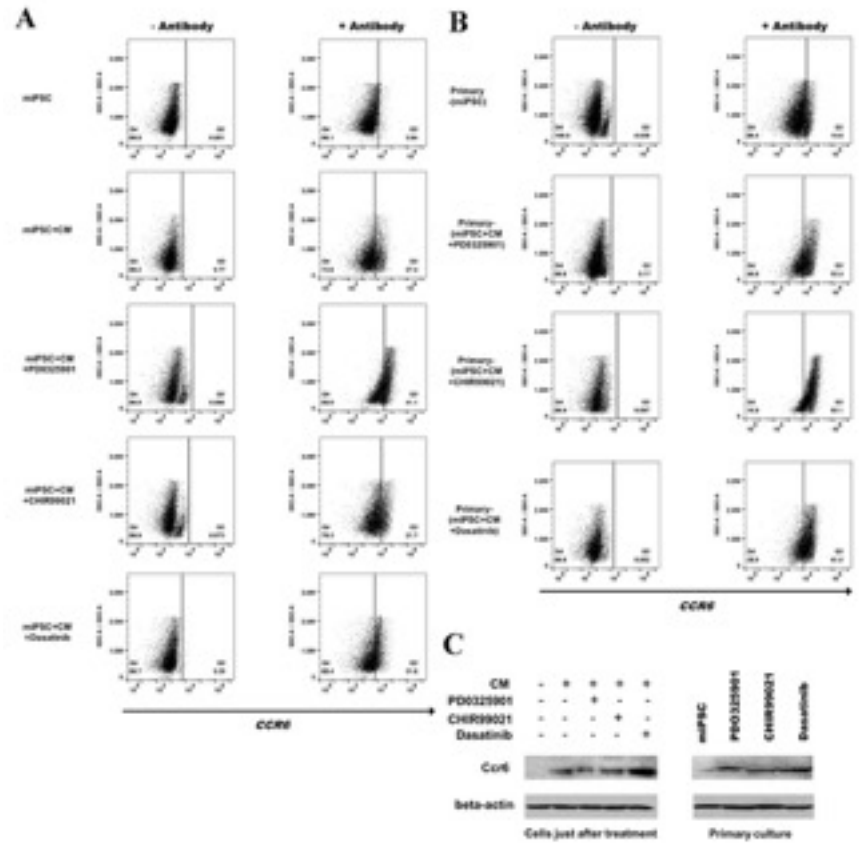

Fig. 4.4. CCR6 expression in converted cells and primary cells by flow cytometry and western blotting. (A) Flow cytometry analysis shows CCR6 population in the converted cells after treated with chemical compounds. (Left: relative expression of cells without treatment by CCR6 (control). (Right: relative expression of cells with treatment by CCR6) (B) Flow cytometry analysis shows CCR6 population in the primary cells. (Left: relative expression of cells without treatment by CCR6 (control). (C)The level of Ccr6-related protein was analyzed by Western blotting. beta-actin served as a loading control.

In conclusion, our study suggested that the presence of CCR6/CCL20/IL17 axis in the CSCs converted from miPSCs and that CCR6 as one of GPCRs, which was the possible target of therapy and/or prevention of cancer.

References

(1) Rosen JM, Jordan CT. The increasing complexity of the cancer stem cell paradigm. Science. **324** (2009) 1670-1673.

(2) Sallusto F, Baggiolini M. Chemokines and leukocyte traffic. Nat Immunol (2008) **9**:949-52.

(3) Chen L, Kasai T, Li Y, Sugii Y, Jin G, Okada M, Vaidyanath A, Mizutani A, Satoh A, and Kudoh T, et al. A model of cancer stem cells derived from mouse induced pluripotent stem cells. PLoS One. **7** (2012) e33544.

(4) Calle AS, Nair N, Oo AKK, Prieto-Vila M, Koga M, Khayrani AC, Zahra MH, Hurley L, Vaidyanath A, and Seno A, et al. A new PDAC mouse model originated from iPSCs-converted pancreatic cancer stem cells (CSCcm). Am J Cancer Res. **6** (2016) 2799-2815.

(5) Nair N, Calle AS, Zahra MH, Prieto-Vila M, Oo AKK, Hurley L, Vaidyanath A, Seno A, Masuda J, and Iwasaki Y, et al. A cancer stem cell model as the point of origin of cancer-associated fibroblasts in tumor microenvironment. Sci Rep. **7** (2017) 6838.

(6) Du J, Xu YN, Saki S, Oo AKK, Hassan G, et al. Signaling Inhibitors Accelerate the Conversion of iPS Cells into Cancer Stem Cells in Tumor Microenvironment. (2019) (under review)

(7) Varona R, Zaballos A, Gutierrez J, Martin P, Roncal F, Albar JP, et al. Molecular cloning, functional characterization and mRNA expression analysis of the murine chemokine receptor CCR6 and its specific ligand MIP-3alpha. FEBS Lett. **440** (1998) 188-194.

(8) Liao F, Alderson R, Su J, Ullrich SJ, Kreider BL, Farber JM. STRL22 is a receptor for the CC chemokine MIP-3alpha. Biochem Biophys Res Commun. **236** (1997) 212-217.

(9) Baba M, Imai T, Nishimura M, Kakizaki M, Takagi S, Hieshima K, et al. Identification of CCR6, the specific receptor for a novel lymphocyte-directed CC chemokine LARC. J Biol Chem. **272** (1997) 14893-14898.

(10) Starner TD, Barker CK, Jia HP, Kang Y, McCray PB Jr. CCL20 is an inducible product of human airway epithelia with innate immune properties. Am J Respir Cell Mol Biol. **29**(2003) 627-633.

(11) Sophie Kirshberg, Uzi Izhar, Gail Amir. Involvement of CCR6/CCL20/IL-17 Axis in NSCLC Disease Progression. **6** (2011) e24856.

(12) Annunziato F, Cosmi L, Santarlasci V, Maggi L, Liotta F, et al. Phenotypic and functional features of human Th17 cells. J Exp Med. **204** (2007) 1849-1861.

(13) Chen Z, O'Shea JJ. Th17 cells: a new fate for differentiating helper T cells. Immunol Res **41**(2008) 87-102.

(14) Kirshberg S, Izhar U, Amir G, Demma J, et al. Involvement of CCR6/CCL20/IL-17 Axis in NSCLC Disease Progression. PLoS one. **9** (2011) e24856.

(15) Hirota K, Yoshitomi H, Hashimoto M, Maeda S, Teradaira S, Sugimoto N, Yamaguchi T, Nomura T, Ito H, Nakamura T, Sakaguchi N, Sakaguchi S. Preferential recruitment of CCR6-expressing Th17 cells to inflamed joints via CCL20 in rheumatoid arthritis and its animal model. J Exp Med. **204** (2007) 2803-2812.

(16) Harper, EG, Guo CS, Rizzo H, Lillis JV, Kurtz SE, et al. Th17 Cytokines Stimulate CCL20 Expression in Keratinocytes In Vitro and In Vivo: Implications for Psoriasis Pathogenesis. J Invest Dermatol. **129** (2009) 2175-2183.

(17) Hirata T, Osuga Y, Takamura M, Kodama A, Hirota Y, et al. Recruitment of CCR6-Expressing Th17 Cells by CCL 20 Secreted from IL-1β, TNF-α, and IL-17A-Stimulated Endometriotic Stromal Cells. Endocrinology. **151** (2010) 5468-5476.

(18) Okita K, Ichisaka T and Yamanaka S. Generation of germline-competent induced pluripotent stem cells. Nature **448** (2007) 313-317.

(19) Ying Q L, Wray J, Nichols J, et al. The ground state of embryonic stem cell self-renewal. Nature. **453** (2008) 519-523.

(20) Tuoya, Sugii Y, Satoh H, Yu DW, Matsuura Y, Tokutaka H, Seno M. Spherical self-organizing map as a helpful tool to identify category-specific cell surface markers. BBRC. **376** (2008) 414-418.

(21) Seno A, Maruhashi T,Kaifu T, Yabe R, Fujikado N, Ma Guangyu,Ikarashi T, Kakuta S, Iwakura Y. Exacerbation of experimental autoimmune encephalomyelitis in mice deficient for DCIR, an inhibitory C-type lectin receptor. Exp Anim. **64** (2015)109-19.

(22) Seno A, Kasai T, Ikenda M, Vaidyanath A, Masuda J, Mizutani A, Murakami H, Ishikawa T, Seno M. Characterization of Gene Expression Patterns among Artificially Developed Cancer Stem Cells Using Spherical Self-Organizing Map. Cancer Inform.**15** (2016) 163-178.

(23) Homey B, Dieu-Nosjean MC, Wiesenborn A, Massacrier C, Pin JJ, Oldham E, et al. Up-regulation of macrophage inflammatory protein-3 alpha/CCL20 and CC chemokine receptor 6 in psoriasis. J Immunol. **164** (2000) 6621-6632.

(24) Kao CY, Huang F, Chen Y, Thai P, Wachi S, Kim C, et al. Up-regulation of CC chemokine ligand 20 expression in human airway epithelium by IL-17 through a JAK-independent but MEK/NF-κB dependent signaling pathway. J Immunol. **175** (2005) 6676-6685.

(25) Yamazaki T, Yang XO，Chung Y, Fukunaga A, Nurieva R, Pappu B, Martin-Orozco N, Kang HS, Ma L, Panopoulos AD, et al. CCR6 regulates the migration of inflammatory and regulatory T cells. J. Immunol. **181** (2008) 8391-8401.

(26) Pan B, Che D, Cao J, Shen J, Jin S, Zhou Y, Liu F, Gu K, Man Y, Shang L, et al. Interleukin-17 levels correlate with poor prognosis and vascular endothelial growth factor concentration in the serum of patients with non-small cell lung cancer. Biomarkers. **20** (2015) 232-239.

(27) Pan B, Shen J, Cao J, Zhou Y, Shang L, Jin S, Cao S, Che D, Liu F, Yu Y. Interleukin-17 promotes angiogenesis by stimulating VEGF production of cancer cells via the STAT3/GIV signaling pathway in non-small-cell lung cancer. Sci. Rep. **5** (2015) 16053-16066.

(28) Raynaud CM, Mercier O, Dartevelle P, Commo F, Olaussen KA, de Montpreville V, Andre F, Sabatier L, Soria JC. Expression of chemokine receptor CCR6 as a molecular determinant of adrenal metastatic relapse in patients with primary lung cancer. Clinic Lung Cancer. **11** (2010) 187-191.

(29) Sutherland A, Mirjolet JF, Maho A, Parmentier M. Expression of the chemokine receptor CCR6 in the Lewis lung carcinoma (LLC) cell line reduces its metastatic potential in vivo. Cancer Gene Ther. **14** (2007) 847-857.

(30) Ghadjar P, Rubie C, Aebersold DM, Keilholz U. The chemokine CCL20 and its receptor CCR6 in human malignancy with focus on colorectal cancer. Int J Cancer. **125** (2009) 741-745.

Materials and Methods

1. Materials

Mouse induced pluripotent stem cells (miPSCs, iPS-MEF-Ng-20D-17; Lot No.012) were provided by the RIKEN Cell Bank, Japan. DMEM, 2-mercaptoethanol, collagenase, gelatin, Hematoxylin and Eosin Y were purchased from Sigma, NY. EBM®-2 media Endothelial cell basal medium-2 and EBM™-2 SingleQuots® Kit were produced from Lonza, MD, USA. MatriGel was acquired from Corning Inc., Corning, NY, USA. KnockOut™ Serum Replacement (KSR) and Non-Essential Amino acids (NEAA) were produced from Gibco, NY. L-Glutamine, 2.5 % Trypsin and $CaCl_2$ were obtained from Nacalai Tesque, Japan. Paraformaldehyde, Hank's balanced salt solution (HBSS) and 100 U/ml penicillin/streptomycin (P/S) cocktail were from Wako, Japan. Leukemia inhibitory factor (LIF) was obtained from Millipore, MA. Mitomycin C treated mouse embryonic fibroblasts (MEF) were provided by Reprocell, Japan. Mouse Lewis lung carcinoma (LLC) cells were obtained from ATCC, VA, USA. Insulin-transferrin-selenium-X (ITS-X) was produced from Life technologies, CA. Signal transduction inhibitors used in this study were obtained as listed in Table 2.2.

Anti-mouse Ki67 rabbit polyclonal antibody (ab15580), anti-mouse Sox2 rabbit polyclonal antibody (ab97959) and anti-mouse panCK rabbit polyclonal antibody (ab191208) were purchased from Abcam, UK. Anti-mouse Akt rabbit

polyclonal antibody (9272), anti-mouse pAkt (Ser^{473}) rabbit polyclonal antibody (9271), anti-mouse Nanog rabbit polyclonal antibody (4903), anti-mouse β-actin rabbit polyclonal antibody (4970), horseradish peroxidase (HRP)–conjugated anti-rabbit IgG goat polyclonal antibody (7074) or anti-mouse IgG goat polyclonal antibody (7076) were purchased from Cell Signaling Technology, MA, USA. Anti-mouse Oct3/4 mouse polyclonal antibody (5279) was purchased from Santa Cruz, CA, USA.

2. Cell Culture

miPSCs were maintained in DMEM supplemented with 15% FBS, 0.1 mM NEAA, 2 mM L-Glutamine, 50 U/ml P/S, 0.1 mM 2-mercaptoethanol and 1000 U/ml of LIF on feeder layers of mitomycin C treated MEF. In the case of feeder-free, the miPSCs were cultured on gelatin-coated dishes. LLC cells were maintained in DMEM containing 10% FBS supplemented with 100 U/ml P/S.

For the primary culture, the mouse allografts were excised and cut into small pieces (approximately 1 mm3) and washed with HBSS three times. These pieces were transferred into a 15-ml tube with 4 ml of dissociation buffer prepared as PBS containing 0.25% trypsin, 0.1% collagenase, 20% KSR, 1 mM of CaCl2 and incubated at 37°C for 40 mins. To terminate the digestion, 5 ml of DMEM containing 10% FBS was then added. The cellular suspension was transferred into the new tubes and centrifuged at 1000 rpm for 5 mins. The cell pellet was resuspended in 5 ml HBSS, and centrifuged at 1000 rpm for 5 min. The cell pellet

was then placed into an appropriate volume of miPS medium without LIF and the cells were seeded into a dish at a density of 5×10^5/ml. The primary cells derived from the mouse allografts were treated with puromycin for 24h to remove the host cells.

To prepare the CM from LLC cells, the medium was collected as previously described (16). The mixture of CM and miPS medium (1:1) was supplemented with each signal inhibitor (Table S2). The miPSCs were cultured in the mixed medium without LIF and MEF feeder cells. One half of the medium was replaced with fresh mixed medium every day, up to day 6. On day 7, the expression of green fluorescent protein (GFP) and cell morphology was observed and photographed using an inverted fluorescent microscope (Olympus IX81, Japan). miPSCs were maintained in DMEM supplemented with 15% FBS, 0.1mM NEAA, 2mM L-Glutamine, 50 U/ml P/S, 0.1mM 2-mercaptoethanol and 1000 U/ml of LIF on feeder layers of mitomycin C treated MEF. In the case of feeder-free, the miPS cells were cultured on gelatin-coated dishes. LLC cells were maintained in DMEM containing 10% FBS supplemented with 100 U/ml P/S.

3. Green fluorescent protein (GFP) Assay

The miPSCs were seeded at a density of 2×10^3 cells/well in 96-well black plates (Corning Inc., NY) and cultured in miPS medium overnight. On the second day, half of the medium was replaced with fresh mixed medium every day, up to day 6. On day 7, the cells were washed twice with PBS and lysed in 50 μl/well lysis

buffer followed by the incubation at 37°C for 5mins. The relative fluorescence intensity was then measured at 509 nm, excited at 488nm, using a microplate reader (SH-9000lab, Corona, Japan). The read of each well was obtained from 9 points at a distance of 1 mm from the bottom of each well flashed 30 times.

The GFP fluorescence from the miPSCs cultured in CM without signal inhibitors was used as the standard to determine the threshold of the bottom line in order to distinguish effect of the signal inhibitors. The fluorescence from 6 wells was measured 5 times from independent experiments, and the averages and standard deviations of read were calculated (Table S1). Next, we assessed the effect of the inhibitors in concentrations between 0 and 10 μM by the intensity of the GFP fluorescence and determined the optimal concentration which enhanced the fluorescence of GFP (Table 2.2).

4. Sphere Formation Assay

The single cells were seeded a density of 1×10^4 cells/well into 24-well ultra-low attachment plates (Corning Inc., NY) in serum free medium consisting of 97.5 % DMEM, 0.5 U/ml P/S, 0.1 mM NEAA, 1 mM L-Glutamine, 0.1 mM 2-mercaptoethanol and 1% v/v ITS-X. After 5 to 7 days, the number of spheroids were counted, and images were captured using an inverted microscope (CKX41, Olympus, Japan) or an inverted fluorescent microscope (IX81, Olympus, Japan).

5. Tube Formation Assay

Cells were seeded in 60 mm dishes, at a density of 5×10^5 cells/dish, and incubated at 37 °C with 5% CO2 until the formation of a 70% confluent monolayer. Next, 5×10^5 cells were collected and resuspended in EBM-2 media and seeded in 12-well plates coated with seeded in growth factors reduced MatriGel for 24h in the presence of human Epidermal Growth Factor (EGF, 5 ng/mL), human Vascular Endothelial Growth Factor (VEGF, 0.5 ng/mL), R3-Insulin-like Growth Factor-1 (R3-IGF-1, 20 ng/mL), Ascorbic Acid (1 µg/mL), Hydrocortisone (0.2 µg/mL), human basic Fibroblast Growth Factor (bFGF, 10 ng/mL), Heparin (22.5 µg/mL) and 2% Fetal Bovine Serum (FBS). The experiments were performed in triplicate and the images of the formed tubes were captured using an Olympus IX81 microscope (Olympus, Tokyo, Japan).

6. Animal Experiments

The plan of animal experiments were reviewed and approved by the ethics committee for animal experiments of at the Okayama University under the IDs OKU-2013252, OKU-2014157, OKU-2014429 and OKU-2016078. All experiments were performed according to the Policy on the Care and Use of the Laboratory Animals, Okayama University. Nude mice (Balb/c-nu/nu, female, 4 weeks) were purchased from Charles River, Japan. Cells at $1x10^6$ were suspended in 200 µl of HBSS and were subcutaneously transplanted into nude mice.

7. RNA Extraction, cDNA Synthesis and reverse transcription quantitative PCR Analysis

Total RNA was extracted from cells using RNAeasy Mini kit (QUIAGEN, Germany) according to the manufacturer's instructions and 1 μg of RNA was reverse transcribed using the Superscript First-Strand kit (Invitrogen, CA). Reverse transcription quantitative PCR (rt-qPCR) was performed with SYBR green I Master Mix (Roche, Switzerland) using LightCycler® 480 Instrument (Roche, Switzerland) according to manufacturer's instructions. The primers used for rt-qPCR are listed in Table. S1.

8. Histological Analysis and Immunohistochemistry

For histological analysis, tumors were excised from the mice 4-6 weeks after transplantation. The paraffin-embedded tissue samples were cut into 5 μm-thickness sections, deparaffinized and stained with 0.5% Hematoxylin and Eosin Y (HE). The primary antibodies and dilutions used for IHC were as follows: 1:200 of anti-Ki67 antibody, 1:200 of anti-Sox2 antibody and 1:200 of anti-panCK antibody.

9. Western Blotting

Proteins extracted from the miPSCs treated with each condition were subjected to SDS-PAGE, transferred to Immobilon®-FL transfer membrane (PVDF, Merck Millipore, Germany) and probed with antibodies against Akt at the dilution of 1:1000, pAkt (Ser^{473}) at the dilution of 1:1000, Oct3/4 at the dilution of 1:3000 and Nanog at the dilution of 1:2000, β-actin1:1000. This was followed by secondary

antibody, either HRP–conjugated anti-rabbit or anti-mouse IgG at the dilution of 1:2,000 or 1:5,000, respectively.

10. Flow cytometry

The miPSCs that survived following the 1-week treatment were transferred 60-mm dish and harvested during the logarithmic growth phase. The cells were re-suspended in 100 μl of ice-cold PBS and analyzed by a flow cytometer (BD Accuri™ C6 plus, Becton & Dickinson, NJ). Data from each experiment was analyzed by FlowJo software (FlowJo, LLC, Ashland, OR, USA).

11. Statistical Analysis

The fluorescence data read by the microplate reader were analyzed using the two-tailed student's t-test and presented as the mean ± standard deviation (SD) from independent experiments repeated at least three times. The statistical significance in mean values between two groups was determined by 2-tailed student's t-test and expressed as the mean value. In the data acquired from the rt-qPCR analysis, the statistical significance between the mean values of more than two groups was determined using one-way analysis of variance (ANOVA) and Dunnett's multiple comparisons test. $P<0.05$ was considered statistically significant.

Table S1. List of Primers Used in the Experiments

NO.	Names	ACCESSION	Forward Primer Sequence 5'- 3'	Reverse Primer Sequence 5'- 3'
1	mouse Oct3/4 endogeneous	NM_013633.2	*TCTTTCCACCAGGCCCCCGGCTC*	*TGCGGGCGGACATGGGGAGATCC*
2	mouse Sox2 endogeneous	NM_011443.3	*TAGAGCTAGACTCCGGGCGATGA*	*TTGCCTTAAACAAGACCACGAAA*
3	mouse Klf4 endogeneous	NM_010637.3	*GGACTTACAAAATGCCAAGGGGTG*	*TCGCTTCCTCTTCCTCCGACACA*
4	mouse c-myc endogeneous	NM_010849.4	*TGACCTAACTCGAGGAGGAGCTGGAATC*	*AAGTTTGAGGCAGTTAAAATTATGGCTGAAGC*
5	mouse Oct3/4 total	NM_013633.2	*CTGAGGGCCAGGCAGGAGCACGAG*	*CTGTAGGGAGGGCTTCGGGCACTT*
6	mouse Sox2 total	NM_011443.3	*GGTTACCTCTTCCTCCCACTCCAG*	*TCACATTGTCGACAGGGGCAG*
7	mouse Klf4 total	NM_010637.3	*CACCATGGACCCGGGCGTGGCTGCCAGAAA*	*TTAGGCTGTTCTGGGCCGGGGCCACGA*
8	mouse c-myc total	NM_010849.4	*CAGAGGAGGAACGAGCTGAAGCGC*	*TTATGCACCAGAGTTTCGAAGCTGTTCG*
9	mouse Oct3/4 transgene	M34381.1	*TTGGGCTAGAGAAGGATGTGGTTC*	*TTATCGTCGACCACTGTGCTGCTG*
10	mouse Sox2 transgene	NM_003106.4	*GGTTACCTCTTCCTCCCACTCCAG*	*TTATCGTCGACCACTGTGCTGCTG*
11	mouse Klf4 transgene	XM_021200389.1	*GCGAACTCACACAGGCGAGAAACC*	*TTATCGTCGACCACTGTGCTGCTG*
12	mouse c-myc transgene	NM_010637.3	*CAGAGGAGGAACGAGCTGAAGCGC*	*TTATCGTCGACCACTGTGCTGCTG*

13	mouse Nanog	NM_028016.3	*AGGGTCTGCTACTGAGATGCTCTG*	*CAACCACTGGTTTTTCTGCCACCG*
14	Pik3ca	NM_008839.2	*GCCACAGACACTACTGCGTA*	*CACCGAACAGCAAAACTCCG*
15	Pik3cb	NM_029094.3	*CTGATTTTACGGCGGCATGG*	*TGAGGGCCTCGTCAAACTTC*
16	Pik3cg	NM_001146201	*ACCTGTGCCTTCTGCCTTAC*	*TGCGGCCTGAAACTTTTCTTC*
17	Pik3r1	NM_001024955.2	*AGCGGAGAACCTATTGCGAG*	*ACTTCGCCGTCTACCACTAC*
18	Pik3r5	NM_177320.2	*AAGTCCTTTGTCAGCAGTCCC*	*CTGGTAAACCTGCAGCAACAC*
19	Pik3r6	NM_001004435.3	*TGAGACGACCACATCCTCCC*	*TCCACATGCCCTGATTGCTC*
20	Pik3ap1	NM_031376.4	*GAAGGCCATTTCTGAAGATTCTGG*	*TCTCGTCCAGCTTGCATCTC*
21	Pten	NM_001304718.2	*AGCTCAGCATTTTCTGGGCTTCA*	*GTGATGGGCTCTGAGACAGAC*
22	Ccr6	NM_001190334.1	*TGAAGACCATAACCCACCACAG*	*AGCATCTTGTTCTGTTTGTGGAAG*
23	Ccl20	NM_016960.2	*CGACTGTTGCCTCTCGTACA*	*GCTTCATCGGCCATCTGTCT*
24	IL17A	NM_010552	*GGGTCTTCATTGCGGTGGAGAG*	*ATCCCTCAAAGCTCAGCGTGTC*
25	IL17A Receptor	NM_008359.2	*ACAGTTCCCAAGCCAGTTGC*	*TCAGCACGATGACAGATCCC*

Publications

1. Signaling Inhibitors Accelerate the Conversion of iPS Cells into Cancer Stem Cells in the Tumor Microenvironment.

   Juan Du, Yanning Xu, Saki Sasada, Aung Ko Ko Oo, Ghmkin Hassan, Hafizah Mahmud, Apriliana Cahya Khayrani, Md Jahangir Alam, Said M. Afify, Kazuki Kumon, Hager M. Mansour, Neha Nair, Ryo Uesaki, Maram H. Zahra, Akimasa Seno, Nobuhiro Okada, Ling Chen, Ting Yan, Masaharu Seno. Oncology reports.

2. Upregulated Ccl20 and Ccr6 in cancer stem cells converted from mouse iPS cells.

   Juan Du, Akimasa Seno, Saki Sasada, Yanning Xu, Aung Ko Ko Oo, Ghmkin Hassan, Shunsuke Ueno, Said M. Afify, Maram H. Zahra, Nobuhiro Okada, Lin Chen, Xiaoying Fu, Heizo Tokutaka, Ting Yan and Masaharu Seno. Archives of Biochemistry and Biophysics.

3. A Preliminary Study on Activity Mechanism and Identification of an Extract of Pharbitis Purpurea Seeds against Tetranychus Cinnabarinus.

   Juan Du, Lei Zhao, Lan-qing Ma, Yu-bo Liu, Guang-lu Shi, and You-nian Wang. Information Tech. and Agricultural Eng. . 2012. AISC 134, pp. 547-556.

4. Acaricidal Activity of the Oleic Acid Methyl Ester from Pharbitis purpurea Seeds against Tetranychus.

Juan Du, Lei Zhao, Lan-qing MA, Yu-bo Liu, Guang-lu Shi, and You-nian Wang. Information Tech. and Agricultural Eng.. 2012. AISC 134, pp. 621-628.

5. Acarocidal Activity of Methyl Cis-9-hexadecenoate Against Tetranychus cinnabarinus.

   Du Juan, Zhao Lei, Shi Guang-lu, and Wang You-nian. JOURNAL 0F BEIJING UNIVERSITY OF AGRICULTURE. 2010 Apr 25(2): 25-28.

6. Acarocidal Activity of Methyl Linoleate against Tetranychus cinnabarinus.

   Du Juan, Zhao Lei, Shi Guang-lu, and Wang You-nian. Chinese Agricultural Science Bulletin. 2010 Jun 26(6): 247-249.

7. Antifungal Activity of Extracts of Stellera chamaejasme against Botrytis cinerea.

   Lei Zhao, **Juan Du**, Lan-qing Ma, Chun-ya Bu, Yu-bo Liu, Guang-lu Shi, and You-nian Wang. Information Tech. and Agricultural Eng.. 2012. AISC 134, pp. 683-692.

8. Up-Regulation of PI 3-Kinases and the Activation of PI3K-Akt Signaling Pathway in Cancer Stem-Like Cells Through DNA Hypomethylation Mediated by the Cancer Microenvironment.

   Aung Ko Ko Oo, Anna Sanchez Calle, Neha Nair, Hafizah Mahmud, Arun Vaidyanath, Junya Yamauchi, Apriliana Cahya Khayrani, **Juan Du**, Md Jahangir Alam, Akimasa Seno, Akifumi Mizutani, Hiroshi Murakami, Yoshiaki Iwasaki, Ling Chen, Tomonari Kasai, and Masaharu Seno. Translational Oncology, Vol 11, Issue 3, (2018)

9. Targeting of Glioblastoma Stem Cells with Doxorubicin Encapsulated in Chlorotoxin-Conjugated Liposomes.

   Hafizah Mahmud, Tomonari Kasai, Apriliana Cahya Khayrani , Mami Asakura, Aung Ko Ko Oo, **Du Juan**, Arun Vaidyanath, Samah El-Ghlban, Akifumi Mizutani, Akimasa Seno, Hiroshi Murakami, Junko Masuda and Masaharu Seno. International Journal of Molecular Sciences, Volume 19, Issue 3, Pages 3, (2018)

10. Exogenous Cripto-1 suppresses Self-Renewal of Cancer Stem Cell Model.

    Md Jahangir Alam, Ryota Takahashi, Said M. Afify, Aung Ko Ko Oo, Kazuki Kumon, Hend M. Nawara, Apriliana Cahyal Khayrani, **Juan Du**, Maram H. Zahra, Akimasa Seno, David S.Salomon and Masaharu Seno. International Journal of Molecular Sciences, Volume 19, Issue 11, Pages 3345, (2018)

11. Targeting Ovarian Cancer Cells Overexpressing CD44 with Immunoliposomes Encapsulating Glycosylated Paclitaxel.

    Apriliana Cahya Khayrani, Hafizah Mahmud, Aung Ko Ko Oo, Maram H. Zahra, Miharu Oze, **Juan Du**, Md Jahangir Alam, Said M Afify, Hagar A. Abu Quora, Tsukasa Shigehiro, Anna Sanchez Calle, Nobuhiro Okada, Akimasa Seno, Koki Fujita, Hiroki Hamada, Yuhki Seno, Tadakatsu Mandai, Masaharu Seno. International Journal of Molecular Sciences, Volume 20, Issue 5, Pages 1042, (2019)

12. Metastasis of Cancer Stem Cells Developed in the Microenvironment of Hepatocellular Carcinoma.

13. Said M Afify, Ghmkin Hassan, Amira Osman, Anna Sanchez Calle, Hend M Nawara, Maram H Zahra, Samah EL-Ghlban, Hager M Mansour, Md J Alam, **Juan Du**, Hager A Abo Qura, Akimasa Seno, Yoshiaki Iwasaki, Masaharu Seno. Bioengineering. 6(3),73.(2019)

Presentations

1. Analysis of the Conversion of iPSCs into Cancer Stem Cells with Non-mutagenic Chemical Compounds. (Poster presentation)

   Juan Du, Tomonari Kasai, Saki Sasada, Aung Ko Ko Oo, Apriliana Cahya Khayrani, Hafizah Mahmud, Neha Nair, Arun Vaidyanath, Masaharu Seno. Consortium of Biological Sciences 2017, The Molecular Society of Japan, No 40th Annual Meeting (Kobe, 2017.12.07).

2. Non-mutagenic Chemical Compounds Enhance the Conversion of iPSCs into CSCs. (Poster presentation)

   Juan Du, Saki Sasada, Aung Ko Ko Oo, Apriliana Cahya Khayrani, Hafizah Mahmud, Maram Hussien Zahra, Hagar Mansour, Said Afify, Md. Jahangir Alam, Akimasa Seno, Masaharu Seno. The 77th annual meeting of the Japanses cancer association, (Osaka, 2018.09.28).

3. Conditioned Medium of Lewis Lung Carcinoma Cells Mediated the Oncogenic Conversion of iPSCs into Cancer Stem-like Cells Through DNA Hypomethylation with Lung Metastasis. (Poster presentation)

   Aung Ko Ko Oo, Aprilliana Cahya Khayrani, **Juan Du**, Md Jahangir Alam, Akimasa Seno, Yoshiaki Iwasaki, Ling Chen, Masaharu Seno. The 6th JCA-AACR Special Joint Conference (2018), The Latest Advances in Lung Cancer Research; From Basic Science to Therapeutics; July 10-12, (Kyoto 2018).

Acknowledgements

With due respect, I wish to express my sincere gratitude to Prof. Masaharu Seno for giving me the opportunity to pursue research in his laboratory. His constant motivation and guidance in planning and execution of this study are truly appreciated. I am thankful for his presence and support during the entire course of study. Without his enlightening instruction, impressive kindness and patience, I could not complete my study of doctor course and this dissertation. His diligence, will power me not only at present but also at my future work.

I would like to express my sense of gratitude to Associate Professor Dr. Hiroshi Murakami, Associate Prof: Dr. Akimasa Seno, Associate Prof: Dr. Nobuhiro Okada, Dr. Arun Vaidyanath, Dr. Tomonari Kasai, Dr. Maram Zahra and Dr. Akifumi Mizutani, for their helpful support and guidance. I am thankful for their valuable suggestion and discussion during the entire course of study.

I would like to extend my special thanks to Ms. Kaoru Furuse, Ms. Nobue Mukai and Ms. Mami Asakura for their kind guidance and timely assistance that helped me to execute many difficult tasks with ease and perfection.

I am also greatly indebted to Dr. Ling Chen, Dr. Ting Yan, Dr. Xiaoying Fu and Dr. Yanning Xu for their encouragement, technical support and friendliness.

I would like to thank the thesis reviewing committee and co-supervisors, Professor Takashi Ohtsuki and Professor Hiroshi Tokumitsu, they genuinely

deserve much of my gratefulness for their useful comments and kindly reviewing my thesis.

Special thanks should go to Dr. Neha Nair, Dr. Anna Sanchez Calle, Dr. Aung Ko Ko Oo, Dr. Md Jahangir Alam, Dr. Hafizah Mahmud, Dr., Dr. Apriliana Cahya Khayrani, , Dr. Xianglin Zhao, Dr. Ghmkin Hassan, Dr. Kazuki Kumon, Dr. Hager Mansour, Dr. Said Afify, Dr. Hend Nawara, Dr. Hagar Ali, Dr. Sadia, MS. Saki Sasada and all the students of Seno lab for their valuable suggestions, encouragement and friendliness, giving me a wonderful memory.

I would like to express my heartfelt gratitude to my husband, Lei Zhao for being the pillar of my strength and for his boundless encouragement for accomplishing my goals.

It goes without saying that the biggest support has come from my parents who are solely responsible for what I am today. There are no words to describe my gratitude for their blessings and love.

I gratefully acknowledge the funding received towards my Ph.D. from the scholarship of China Scholarship Council.

Juan Du

Okayama University

September 2019